

T-3988

The Beam Optics Study
of the General Ionex Model 1545
Linear Particle Accelerator

By
Lian He

ARTHUR LAKES LIBRARY
COLORADO SCHOOL of MINES
GOLDEN, COLORADO 80401

ProQuest Number: 10783671

All rights reserved

INFORMATION TO ALL USERS

The quality of this reproduction is dependent upon the quality of the copy submitted.

In the unlikely event that the author did not send a complete manuscript and there are missing pages, these will be noted. Also, if material had to be removed, a note will indicate the deletion.



ProQuest 10783671

Published by ProQuest LLC (2018). Copyright of the Dissertation is held by the Author.

All rights reserved.

This work is protected against unauthorized copying under Title 17, United States Code
Microform Edition © ProQuest LLC.

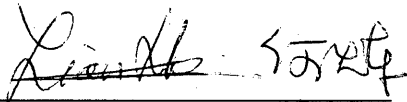
ProQuest LLC.
789 East Eisenhower Parkway
P.O. Box 1346
Ann Arbor, MI 48106 – 1346

T-3988


A thesis submitted to the Faculty and the Board of Trustees of the Colorado School of Mines in partial fulfillment of the requirements for the degree of Master of Science (Physics).

Golden, Colorado

Date: 11-12-90

Signed: 

Lian He

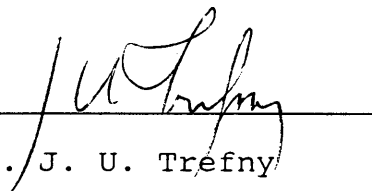
Approved: 

Dr. F. E. Cecil

Thesis Advisor

Golden, Colorado

Date: 11-12-90

Signed: 

Dr. J. U. Trefny

Professor and Head

Physics Department

ABSTRACT

The transport optics of a General Ionex Model 1545 Linear Particle Accelerator is studied by using a scanning type beam profile monitor. The experimental data collected at the target chamber is analyzed to a theoretical model through a FORTRAN code, and the results agree well as the results given by a theoretical accelerator design program OPTICIAN.

TABLE OF CONTENTS

| | Page |
|---------------------------------------|------|
| ABSTRACT | iii |
| LIST OF FIGURES | v |
| LIST OF TABLES | vii |
| ACKNOWLEDGEMENTS | viii |
| Chapter I. INTRODUCTION | 1 |
| Chapter II. BACKGROUND | 4 |
| 2.1 The Accelerator | 4 |
| 2.2 Optical Components | 7 |
| Chapter III. EXPERIMENT | 14 |
| 3.1 Beam Profile Monitor | 14 |
| 3.2 Beam Optics Study | 18 |
| Chapter IV. MODEL FITTING | 26 |
| 4.1 Fitting Data to an Equation | 26 |
| 4.2 Beam Profile Simulation | 34 |
| Chapter V. COMPARISON | 38 |
| REFERENCE CITED | 42 |
| SELECTED BIBLIOGRAPHY | 43 |
| Appendix A. NORMAL DISTRIBUTION | 45 |
| Appendix B. FORTRAN PROGRAM | 48 |

LIST OF FIGURES

| | Page |
|---|------|
| Figure 2-1 The General Ionex Model 1545 Linear Particle Accelerator | 6 |
| Figure 2-2 The Lens Action of a Unipotential Lens | 9 |
| Figure 3-1 The Detector Cross Section View | 15 |
| Figure 3-2 Circuit Diagram of the Multiplexing Electronic | 17 |
| Figure 3-3 Best Voltage Setting of Grid Einzel Lens | 19 |
| Figure 3-4 Adjusting Range of Grid Einzel Lens Voltage | 21 |
| Figure 3-5 Horizontal Beam Profile at 100 KV Accelerating Voltage | 22 |
| Figure 3-6 Horizontal Beam Profile at 50 KV Accelerating Voltage | 23 |
| Figure 3-7 Beam Profile at 100 KV Accelerating Voltage ($V_G = 17.0$ KV) | 24 |
| Figure 3-8 Beam Profile at 50 KV Accelerating Voltage ($V_G = 9.0$ KV) | 25 |
| Figure 4-1 Relative Beam Intensity as Function of n and V_G at 80 KV Accelerating Voltage | 35 |

| | | | |
|------------|--|-------|----|
| Figure 4-2 | Relative Beam Intensity as Function of $\text{Sin}\theta$ and V_g at 80 KV Accelerating Voltage | | 36 |
| Figure 4-3 | Beam Profile at 80 KV Accelerating Voltage ($V_g = 15$ KV) | | 37 |
| Figure 5-1 | Beam Profile Generated by OPTICIAN | | 40 |

LIST OF TABLES

| | Page |
|---|------|
| Table 2-1 Applications of the Accelerator | 5 |
| Table 2-2 Beam Specifications | 7 |
| Table 2-3 Transfer Matrix | 9 |
| Table 4-1 Coefficients of Parameters in Estimate Model | 31 |
| Table 4-2 Coefficients of μ_x in Estimate Model | 32 |
| Table 4-3 Coefficients of Parameters in Predictor Model | 33 |
| Table 4-4 Coefficients of μ_x in Predictor Model | 33 |
| Table 4-5 Performances of Predictor Models | 34 |
| Table 5-1 List Output of OPTICIAN at 100 KV Accelerating Voltage | 39 |

ACKNOWLEDGEMENTS

I would like to appreciate my entire Thesis Committee; Dr. F. Edward Cecil for his long standing encouragement and patience that made this work possible; Dr. James T. Brown for the knowledge which I learned and for his sense of humor which made my college life more colorful; and Dr. William B. Law for his careful consideration of my academic background.

I would also like to thank Mr. Rex Rideout for his help in the electronic circuit design of the beam profile monitor and to thank Mr. Huaizhu Liu for the helpful discussions on this thesis.

Finally, I would like to thank Dr. J. U. Trefny who brought me the opportunity to come to CSM and to thank the Physics department, the Graduate School, and the U. S. Department of Energy for their financial support.

Chapter I

INTRODUCTION

Since Becquerel's discovery of radioactivity in 1896, the experimental and theoretical studies in nuclear physics have played a prominent role in the development of twentieth century physics. From these studies, we have today a reasonably good understanding of properties of nuclei and of the structure that is responsible for those properties.

Laboratory experiments in nuclear physics have been applied to the understanding of an incredible variety of problems, from the interactions of quarks, to the processes that occurred during the early evolution of the universe just after the Big Bang. Today, a good understanding of experimental techniques and the proper use of experimental instruments are even more important for an experimental physicist.

Particle accelerators are the most useful tools for the research in nuclear physics. The beams produced from those machines can be used to disintegrate nuclei, produce new unstable isotopes, and investigate the properties of nuclear forces.

The purpose of an accelerator of charged particles is to bombard a target with a beam of a specific kind of

particles of chosen energy. There are many varieties of methods for accomplishing this task, all using various arrangements of electric and magnetic fields.

As an electronic device, the accelerator requires a source of charged particles, an electric field to accelerate the particles, focusing elements to counteract the natural tendency of the beam to diverge, deflectors to aim the beam in the desired direction, a target chamber to house all the components in high vacuum to prevent the beam from scattering in collisions with molecules in the air.

The design of accelerators varies greatly with the purpose for which they will be used. Some of them are operated at high energy range up to TeV (10^6 MeV), the Tevatron at Fermilab has recently been modified to operate as a proton collider with each beam having an energy 1 TeV; some of them are physically large, the two-mile long 32 GeV linear electron accelerator at Stanford, 2.2 km rings 26 GeV proton synchrotron accelerator at CERN (the Center European for Nuclear Research). Although the details of these accelerators may be rather technically difficult, they have a basic requirement to produce high intensity and well controlled beams which can reduce the statistical error of experimental data and difficulties of accelerator operation. Understanding of the beam optics (or beam transport) system

of an accelerator, which consists of a number of electric and magnetic devices that focus the beam and bend or deflect it along the desired path, becomes more important for the accelerator operation and maintenance.

This thesis will concentrate on the beam optics study of the General Ionex Model 1545 linear particle accelerator. A theoretical beam optics model of the accelerator will be given at full operation conditions.

Chapter II

BACKGROUND

The beam transport in the accelerator is a process in which charged particles interact with the electromagnetic fields produced by the components of the accelerator. To study the process, we should have a good understanding of the accelerator structure and functions of its components.

2.1 The Accelerator

The General Ionex Model 1545 Linear Particle accelerators [GE82] are typical of the experiment tools in low energy nuclear physics since it can produce 0 -180 KeV continuously variable energy high intensity beams. Table 2-1 shows the applications of the accelerator. The accelerator has a simple structure which consists of an ion source, extraction gap, Einzel lens, crossed-field analyzer (or electromagnetic mass analysis magnet), acceleration tube, grid Einzel lens, source pump manifold, and associated power supplies as shown in Figure 2-1.

The basic operation of the accelerator starts at the ion source. Neutral (Hydrogen or Helium for example) gas atoms enter the top of the ion source and are ionized in the

Table 2-1. Applications of the Accelerator [GA89]

| Applications | Features |
|---------------------------------|---------------------------|
| Cross Section Measurements | High Current up to 0.3 mA |
| Plasma Diagnostic | High Beam Stability |
| Ion Implantation | Heavy Ion Capability |
| Low Energy Backscatter Analysis | Wide Energy Range 180 KeV |
| Detector Calibration | Precise Beam Optics |
| Materials Modification | Positive Ions |

vicinity of a hot filament which provides an electron discharge. A strong axial magnetic field produced by a coil around the ion source constricts the ions to a narrow plasma beam along the axis of the exit aperture and also concentrates the electrons leaving the filament to increase the ionizing efficiency. The positively charged ions are then extracted by the extraction gap which is a negative high voltage probe electrode. A divergent initial beam having an energy up to 30 KeV is formed. Then, the beam is focussed by the first Einzel lens and bent by the analyzing magnet to the top of acceleration tube. The impurities, different isotopic species, are separated by the analyzing magnet due to the mass difference. Additional acceleration up to maximum beam energy or deceleration down to minimum

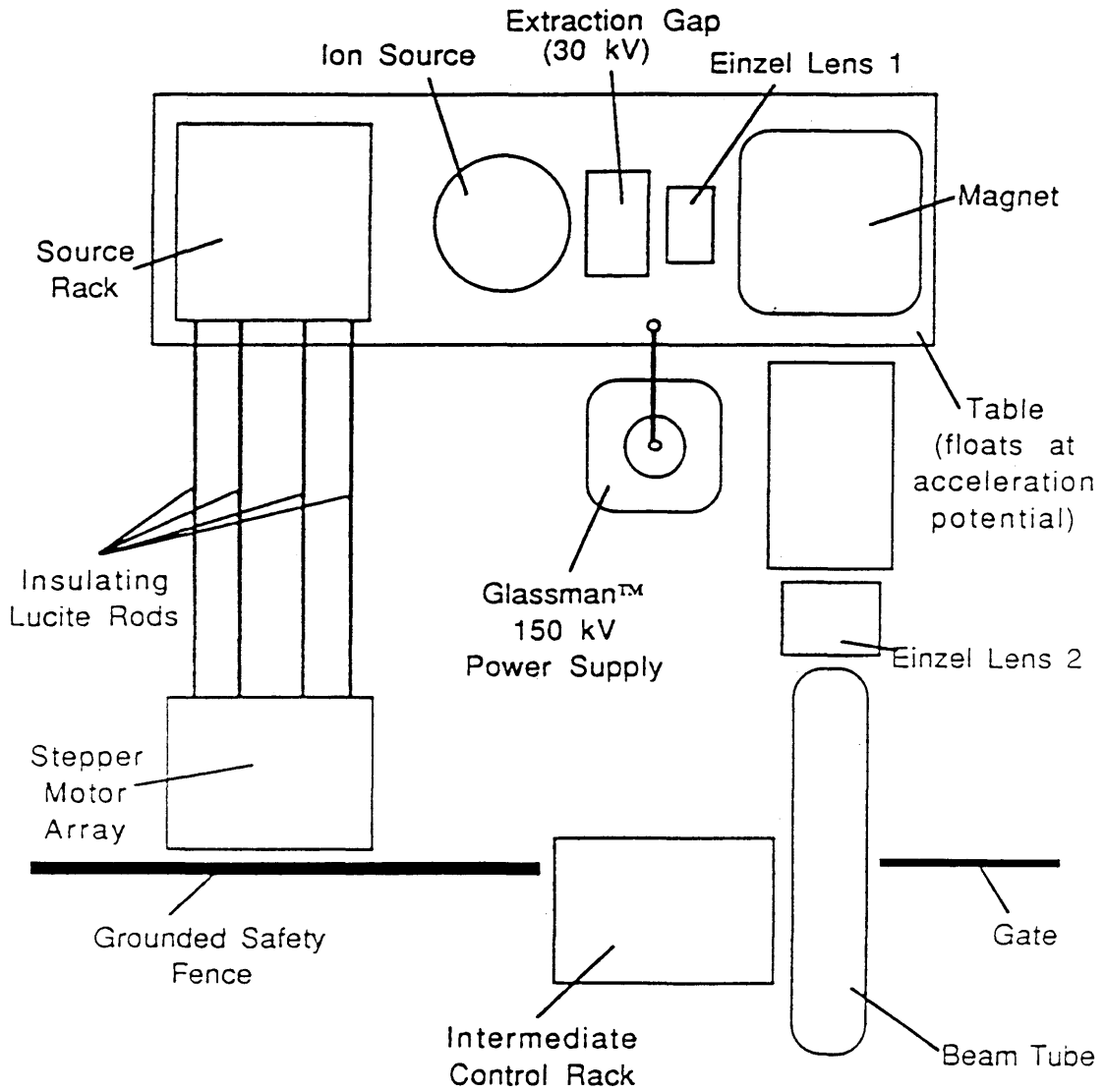


Figure 2-1. General Ionex Model 1545 Accelerator [CE89]

beam energy is provided by the acceleration tube. Finally, the grid Einzel lens focuses the beam to an appropriate size (about 0.4 cm diameter) at the target position for experiments.

After the beam was formed at the ion source, its properties are dependent on the function of the optical components of the accelerator, Einzel lenses and analyzing magnet, that force the beam to a desired path with a designed shape. The better the operating conditions of these components, the better the beam symmetry achieved. Table 2-2 shows the designed beam specifications.

Table 2-2. Beam Specifications [GA89]

| Energy (KV) | Current (μ A) | Divergence (1/2 angle, mrad) |
|-------------|--------------------|------------------------------|
| 150 | 300 | 15 |
| 20 | 150 | 20 |
| 1 | 1 | 100 |

2.2 Optical Components

Charged particle optics is similar to light optics. For geometric light optics it has been customary since the time of Newton to use an algebraic formulation for all equations

involved. However, this method has been replaced in many cases by the use of transfer matrices which offers an unexcelled simplicity and clarity for a complex optical system.

In the matrix representation, we can describe the relationship between image space (2) and object space (1) of a bundle rays passing through an optical system as

$$\begin{bmatrix} r_2 \\ \theta_2 \end{bmatrix} = \begin{bmatrix} m_{11} & m_{12} \\ m_{21} & m_{22} \end{bmatrix} \begin{bmatrix} r_1 \\ \theta_1 \end{bmatrix} \quad (2-1)$$

where r is the distance from the axis of the system (z -axis) and θ is the angle between the rays and the axis.

The matrix $M = [m_{ij}]$ is called transfer matrix of the system. Table 2-3 shows the transfer matrices of some simple optical system.

The great advantage of this method is that we can write a transfer matrix of a complex system as the multiplication of the transfer matrices of each component

$$[M_{\text{total}}] = [M_n] [M_{n-1}] \cdots [M_2] [M_1] \quad (2-2)$$

If each transfer matrix of the component is specified, the optical properties of a system are determined.

We will use the transfer method to study each optical component of the accelerator.

Table 2-3. Transfer Matrix

| Optical System | Transfer Matrix | Commend |
|------------------------|--|---|
| Field Free Drift Space | $\begin{bmatrix} 1 & d \\ 0 & 1 \end{bmatrix}$ | $d = z_2 - z_1$ |
| Plane Boundary | $\begin{bmatrix} 1 & 0 \\ 0 & n_1/n_2 \end{bmatrix}$ | n - index of refraction |
| Spheric Boundary | $\begin{bmatrix} 1 & 0 \\ (n_1/n_2 - 1)/r & n_1/n_2 \end{bmatrix}$ | r - radius of surface |
| Thin Lens | $\begin{bmatrix} 1 & 0 \\ -1/f & 1 \end{bmatrix}$ | $f > 0$ converging $f < 0$ diverging |

The unipotential electrostatic lens (Einzel lens) is a case of three cylinders placed coaxially with the same potential on the two outside cylinders. The focussing fields are derived from voltages applied between three adjacent electrodes, as shown in Figure 2-2.

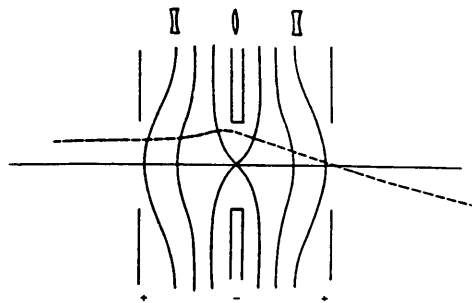


Figure 2-2. The lens Action of a Unipotential Lens

When a ray (consider positive ions only) proceeds in the direction of increasing potential, it experiences a radial electrostatic force caused by the gradient of the potential which decelerates it and pushes it radially away from the axis that is a divergent action. The opposite proceeding is a convergent action. In general, when a ray proceeds in the direction of increasing potential, a concave equipotential has a convergent effect and a convex equipotential has a divergent effect. Since the ions which have a higher energy in a convex equipotential region are exposed for a shorter time to the defocussing field than they are kept in the concave equipotential region where is a focussing field. The net effect is that the positive focusing effect always dominate. It is also true if the ions proceed into an Einzel lens in the direction of decreasing potential. The Einzel lens is always a converging element. The Einzel lens also has an important feature that the beam enters and leaves the lens with the same energy.

Under the assumption that ions move alone to the axis, the paraxial ray equation of motion for an axially symmetric electrostatic field can be written as [BA66]

$$\frac{d^2 r}{dz^2} + \frac{V_0'}{2V_0} \frac{dr}{dz} + \frac{V_0''}{4V_0} r = 0 \quad (2-3)$$

where V_0 is the axial potential. The transfer matrix of an Einzel lens is found by solving Equation (2-3) as

$$M = \begin{bmatrix} \frac{8\sqrt{V_1 V_2 - 3V_1 - 3V_2}}{2(V_1 V_2)^{\frac{1}{2}}} & \frac{2d(3\sqrt{V_2} - \sqrt{V_1})}{V_2 + (V_1 V_2)^{\frac{1}{2}}} \\ \frac{3V_1 - 3V_2}{8d} \cdot \frac{(\sqrt{V_1} - \sqrt{V_2})(3\sqrt{V_1} - \sqrt{V_2})}{(V_1^2 V_2)^{\frac{1}{2}}} & \frac{8\sqrt{V_1 V_2 - 3V_1 - 3V_2}}{2(V_1 V_2)^{\frac{1}{2}}} \end{bmatrix} \quad (2-4)$$

where V_1 is the potential of the outside electrodes, V_2 is the potential of the central electrode and d is the half length of the cylinders.

The grid Einzel lens is a symmetrical Einzel lens with the central electrode replaced by a mesh grid which will give a better optical qualities than the Einzel lens.

The analyzing magnet is also an important optical element for deflection and focussing of charged particles in the accelerator. The magnet can focus the ion beam in either or both radial and vertical planes depending on the field configuration. The separation of the beam is determined by its momentum spread.

In the analyzing magnet, the ions experience the Lorentz force which causes a particular mass to be selected by the magnet. If the magnetic field B is perpendicular to the moving direction of the ions, the selected mass can be

written as

$$m = (qBR)^2 / 2E_0 \quad (2-5)$$

where R is the radius of curvature of the magnet and E_0 is the initial energy of ions before entrance the magnet. For ions having different masses, the paths are different which will affect the optical properties of the beam. Using a relative momentum spread $\Delta P/P$ as a component in the initial and final column vector in addition to r and θ , a transfer matrix for normal entrance into the sector magnet is [LI69]

$$M = \begin{bmatrix} \text{Cos}(\delta\alpha) & R\delta^{-1}\text{Sin}(\delta\alpha) & R\delta^{-2}[1-\text{Cos}(\delta\alpha)] \\ -R^{-1}\delta\text{Sin}(\delta\alpha) & \text{Cos}(\delta\alpha) & \delta^{-1}\text{Sin}(\delta\alpha) \\ 0 & 0 & 1 \end{bmatrix} \quad (2-6)$$

where α is the bending angle of the sector magnet and δ is given by

$$\delta = (1 - n)^{\frac{1}{2}} = \left(1 + \frac{r}{B} \frac{dB}{dr}\right)^{\frac{1}{2}} \quad (2-7)$$

in which n is called the field index. For a uniform B field, n is zero.

The acceleration tube is a multi-electrode structure that imparts energy to the ions in successively stages. As the ions travel along the tube, the increased potential

energy of ions convert to the kinetic energy toward a desired beam energy. Many studies have indicated that the optics of an acceleration tube are essentially linear. It is convenient to represent a tube as a linear system in terms of the transfer matrix.

All of the above discussion neglects the space-charge effect which is produced by the ion beam itself. So, the optical properties of these components of the accelerator are in the paraxial region. At 1 mA of beam current, the space-charge effect is two orders smaller than our result. Since the beam current of the accelerator is less than 1 mA, the approximation of neglecting space-charge effect is appropriate. The higher order optical properties can be obtained either by solving Poisson's equation with the space-charge density ρ at a set of proper boundary conditions exactly or by solving Equation (2-3) adding term of $\rho/(4V_0\epsilon_0)$.

Chapter III

EXPERIMENT

A scanning type beam profile monitor has been designed and installed on the accelerator. Using the beam profile monitor, the final beam patterns were studied. All experiment data were collected at the target chamber through the beam profile monitor when the Extraction Gap voltage was set to 20 KV and the first Einzel Lens voltage was set to 15 KV.

3.1 Beam Profile Monitor

The beam profile monitor consists of a detector and an analog electronic circuit. The detector was made by A. Gaviria [GA89]. The eleven copper rings acting as charge collectors, each has the width of $1/8$ inches separated from one another by $1/32$ inches, are mounted on a ceramic rod which is positioned across a diameter perpendicular to the direction of beam propagation. The cross section view of the detector is shown in Figure 3-1. Each copper ring intercepts an amount of charge that is proportional to the intensity of the beam at that point. Wires from each individual ring were brought out of the target chamber and fed into the switching

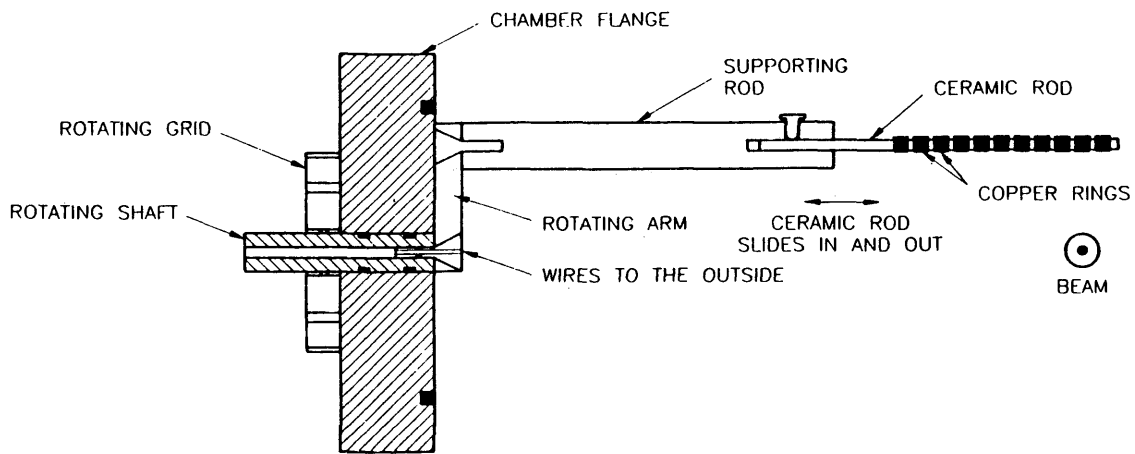


Figure 3-1. The Detector Cross Section View [GA89].

electronic circuit [GA84].

The charge collected by each copper ring is stored in a 1 μ F capacitor (the eleven capacitors were selected for better than 1% match), via a varistor-diode-neon-varistor protection network. The voltage on each capacitor is sampled by an analog multiplexer IC driven at a convenient rate (11 kHz) by a free-running counter. The output of the multiplexer is sent directly to the storage oscilloscope with the time base triggered by the counter and sweep speed set so that one complete scan of the eleven inputs is one sweep. The schematic of switching circuit diagram is shown in Figure 3-2.

The beam profile which can be seen on the scope was divided to eleven channels. Each channel gives the voltage across each 1 μ F capacitor and is proportional to the amount charge collected by each ring. The output of a certain channel represents the relative beam intensity at that point of beam cross section. By rotating the detector crossing the accelerated beam, recording data at each position, a completed beam profile is achieved.

At zero voltage input of the beam profile monitor, the difference of output between channels caused by the leaking current of the diodes is less than 20 mV and is much smaller than the output at normal operation condition, which is

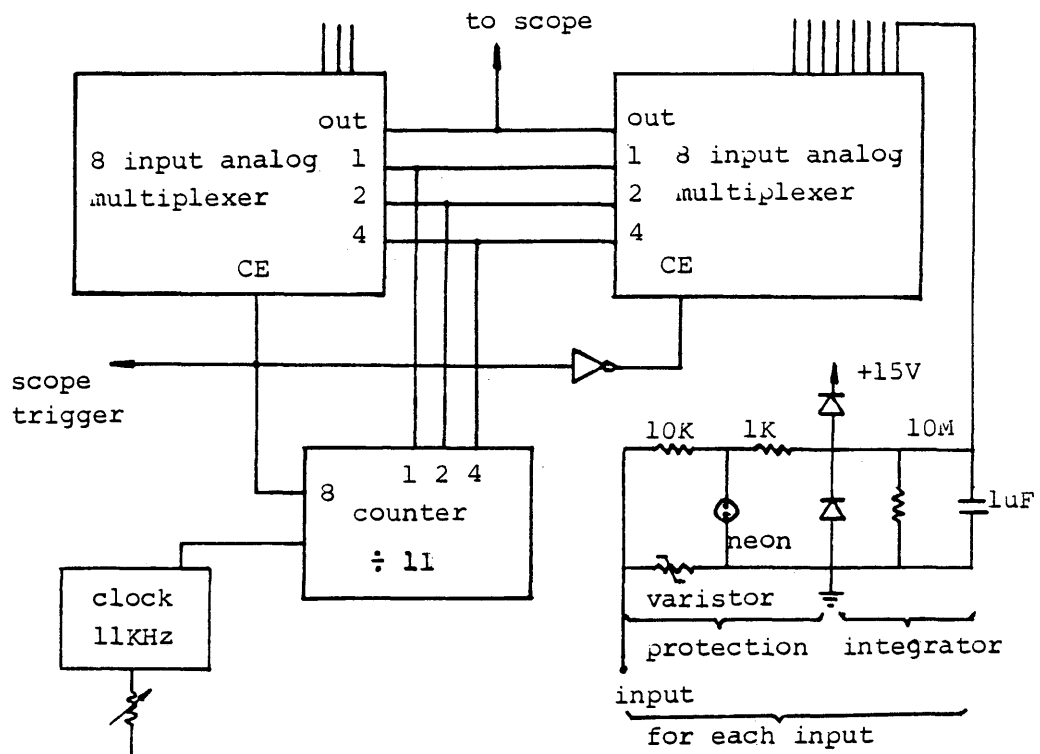


Figure 3-2. Circuit Diagram of Multiplexing Electronics

between 1 to 15 V. The beam profile monitor is tested stable and reliable in the beam current range of the accelerator.

3.2 Beam Profile Study

Two experiments were designed to study the final beam profiles. In the first experiment, the detector was fixed at the center of the target chamber for which y is zero and measured the relative beam intensity as the function of the voltage of the Grid Einzel Lens (GEL), which gives a certain focal strength of the beam, at different accelerating voltage. A best voltage setting of GEL was found for each accelerating voltage which gave the highest symmetric output from beam profile monitor. In the second experiment, we measured the beam profile at the best voltage setting of GEL which we found in the previous experiment at different accelerating voltage. Both experiments were performed when Extraction Gap voltage was set to 20 KV, the voltage of the first Einzel Lens was set to 15 KV and the accelerating voltage was selected at 0 KV, 25 KV, 50 KV, 75 KV and 100 KV.

At the best voltage setting of GEL, we found the highest sharp peak from the beam profile monitor which indicates the best achieved optical properties of the

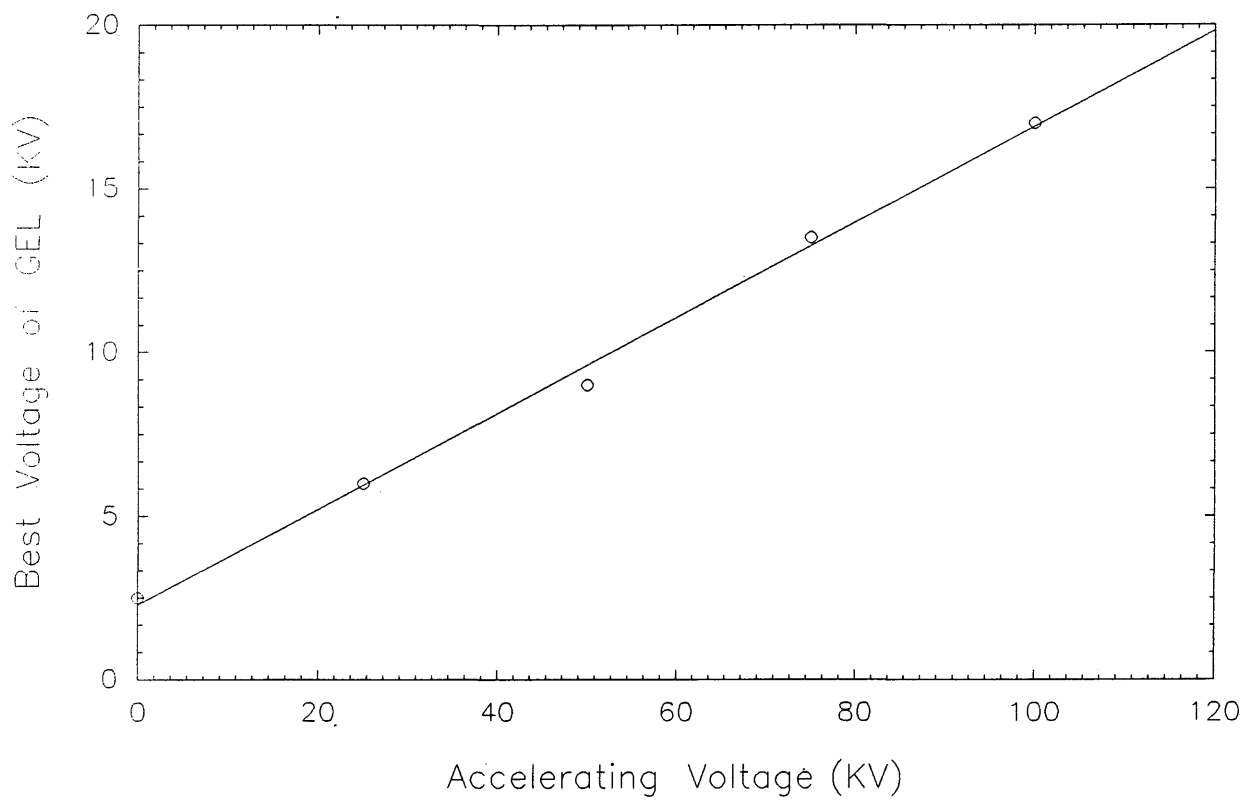


Figure 3-3. Best Voltage Setting of Grid Einzel Lens

accelerator. Figure 3-3 shows the relationship between the accelerating voltage (V_a) and the best voltage setting of GEL (V_g). The good linear regression leads to the linear operation condition of the accelerator.

The beam spreads out as the voltage of GEL goes off its best position. The voltage adjusting range of GEL grows almost linearly as the accelerating voltage increases as shown in Figure 3-4. The horizontal beam profiles are also studied at five different accelerating voltages. Some of them are shown in Figure 3-5 and Figure 3-6 in which we can see clearly the peak moving as a function of GEL voltage. In next chapter, we will find a theoretical model which will represent this kind relationship when y is set to zero.

In the second experiment, we measured five complete beam profiles, some of them are shown in Figure 3-7 and figure 3-8. From these plots, we found that the shape of the beam profile is stable for the studied range of accelerating voltage and the peak of the beam profile is a little bit below the center of the target chamber which may depend on the position setting of the detector.

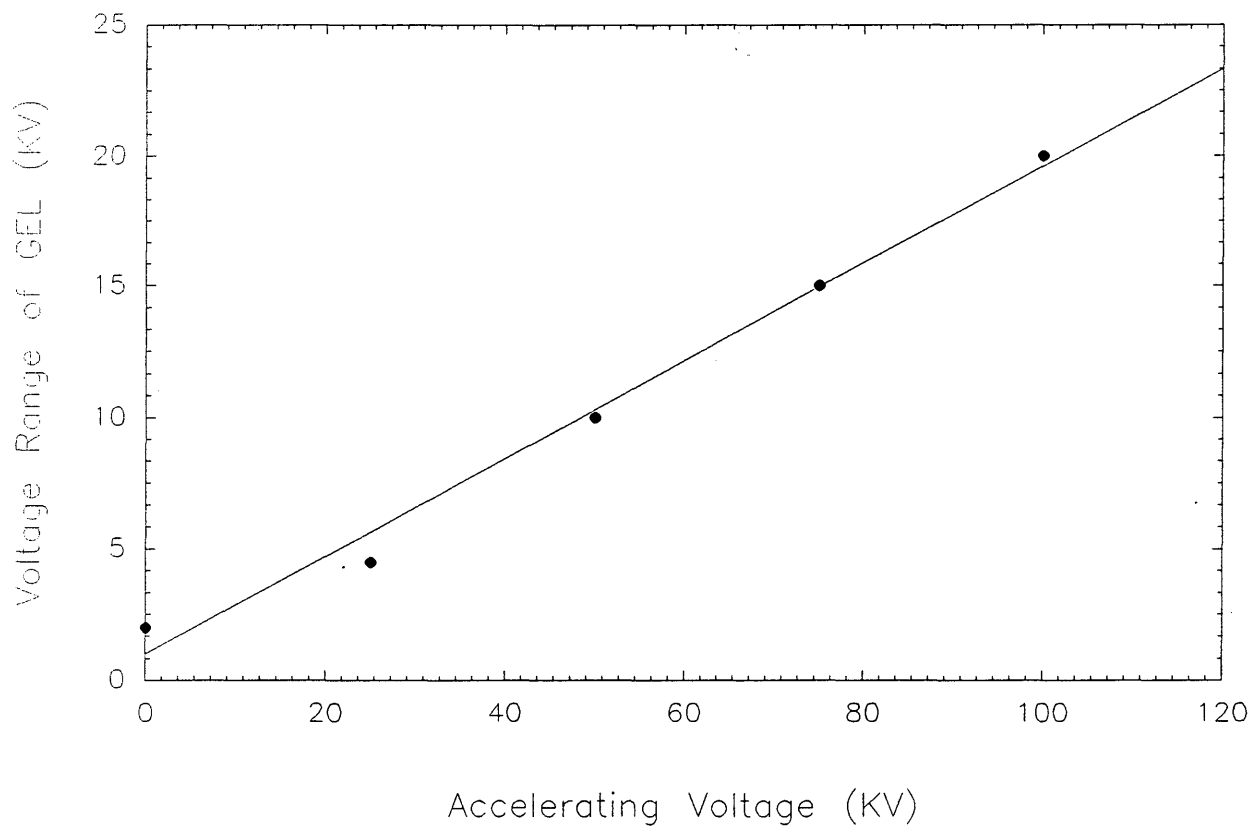
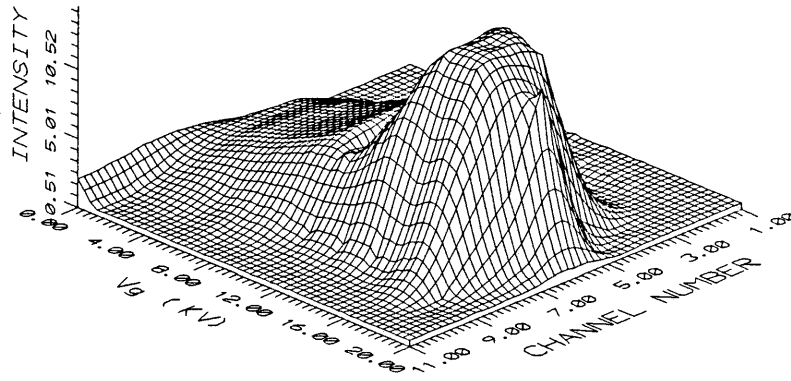


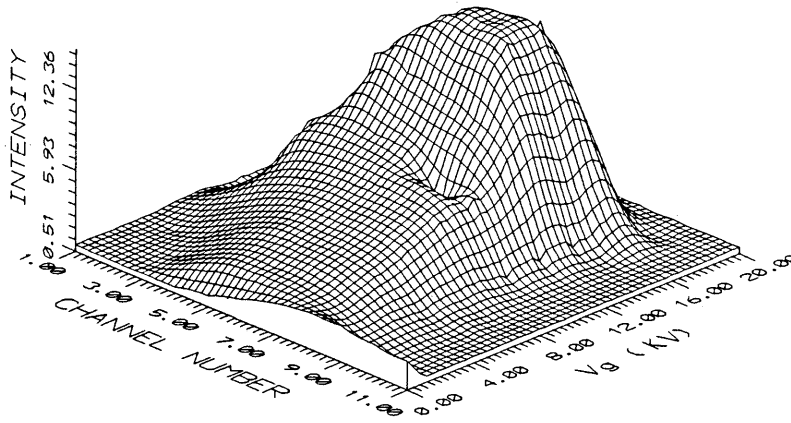
Figure 3-4. Adjusting Range of Grid Einzel Lens Voltage

• 45 DEGREES ROTATION ABOUT Z-AXIS.



(a)

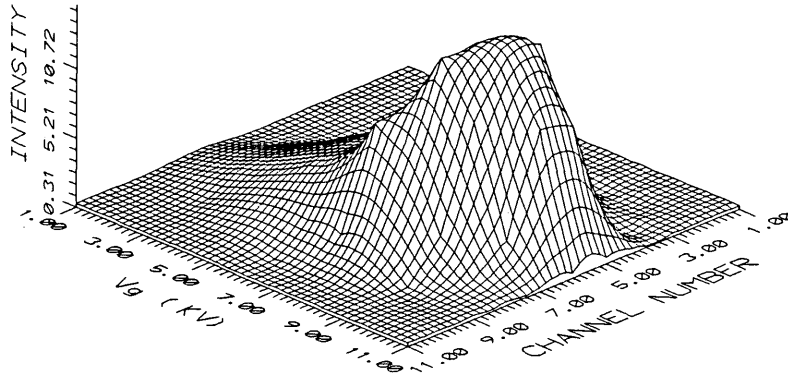
• -45 DEGREES ROTATION ABOUT Z-AXIS.



(b)

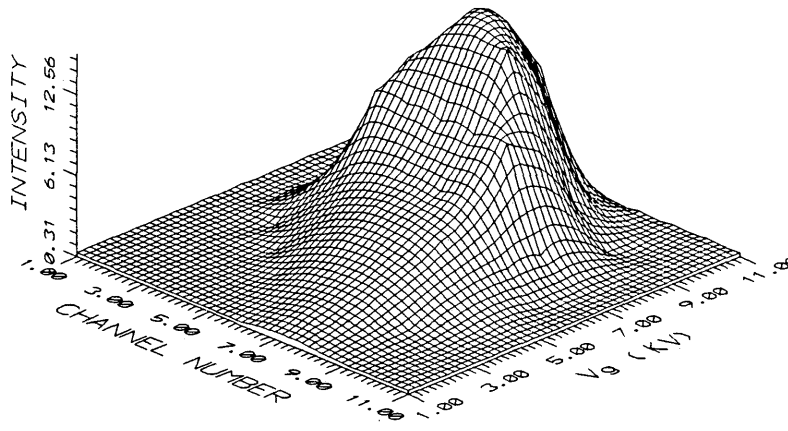
Figure 3-5. Horizontal Beam Profile at 100 KV Accelerating Voltage

* 45 DEGREES ROTATION ABOUT Z-AXIS.



(a)

* -45 DEGREES ROTATION ABOUT Z-AXIS.



(b)

Figure 3-6. Horizontal Beam Profile at 50 KV Accelerating Voltage

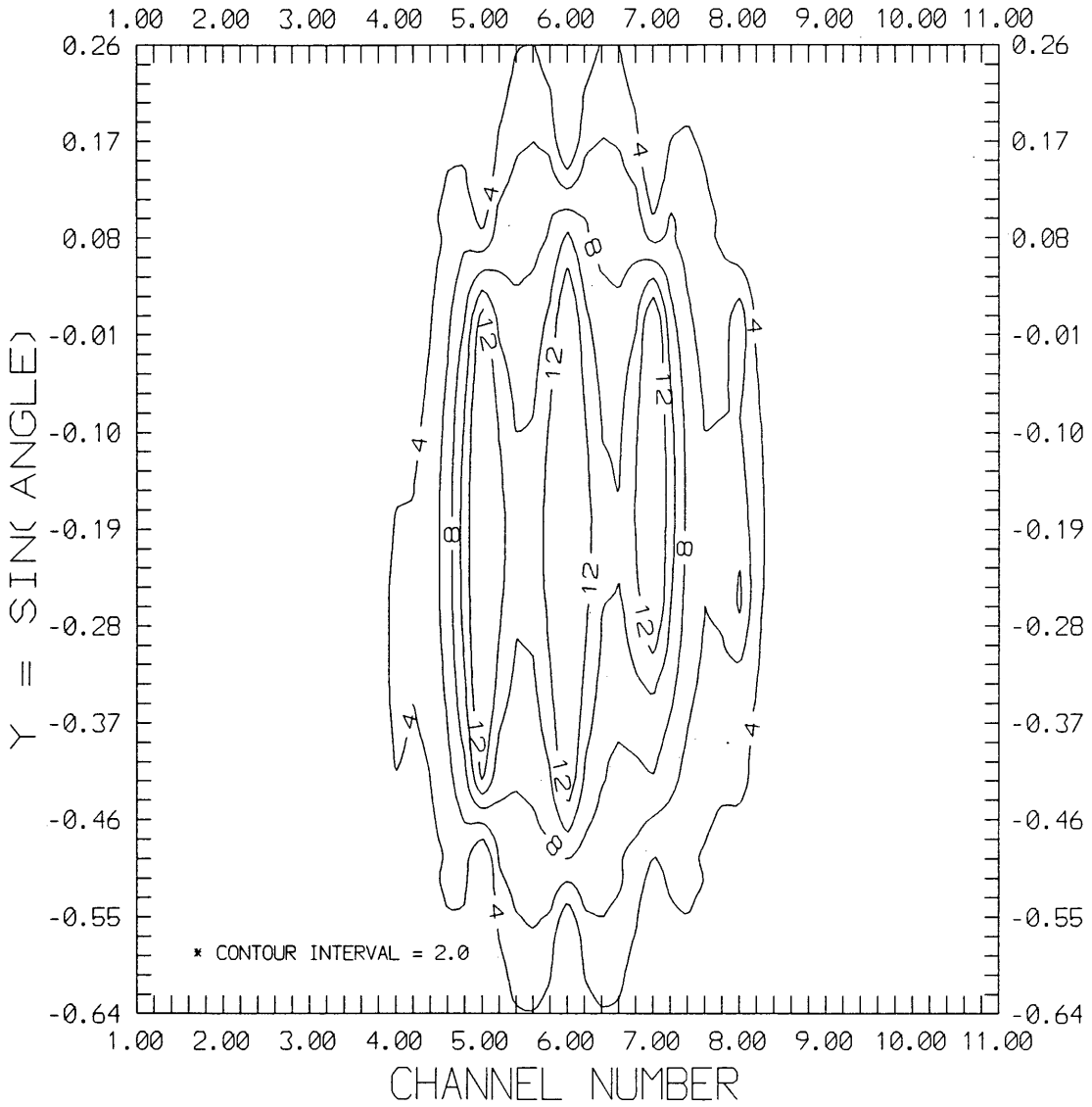


Figure 3-7. Beam Profile at 100 KV Accelerating Voltage.
($V_g = 17.0$ KV)

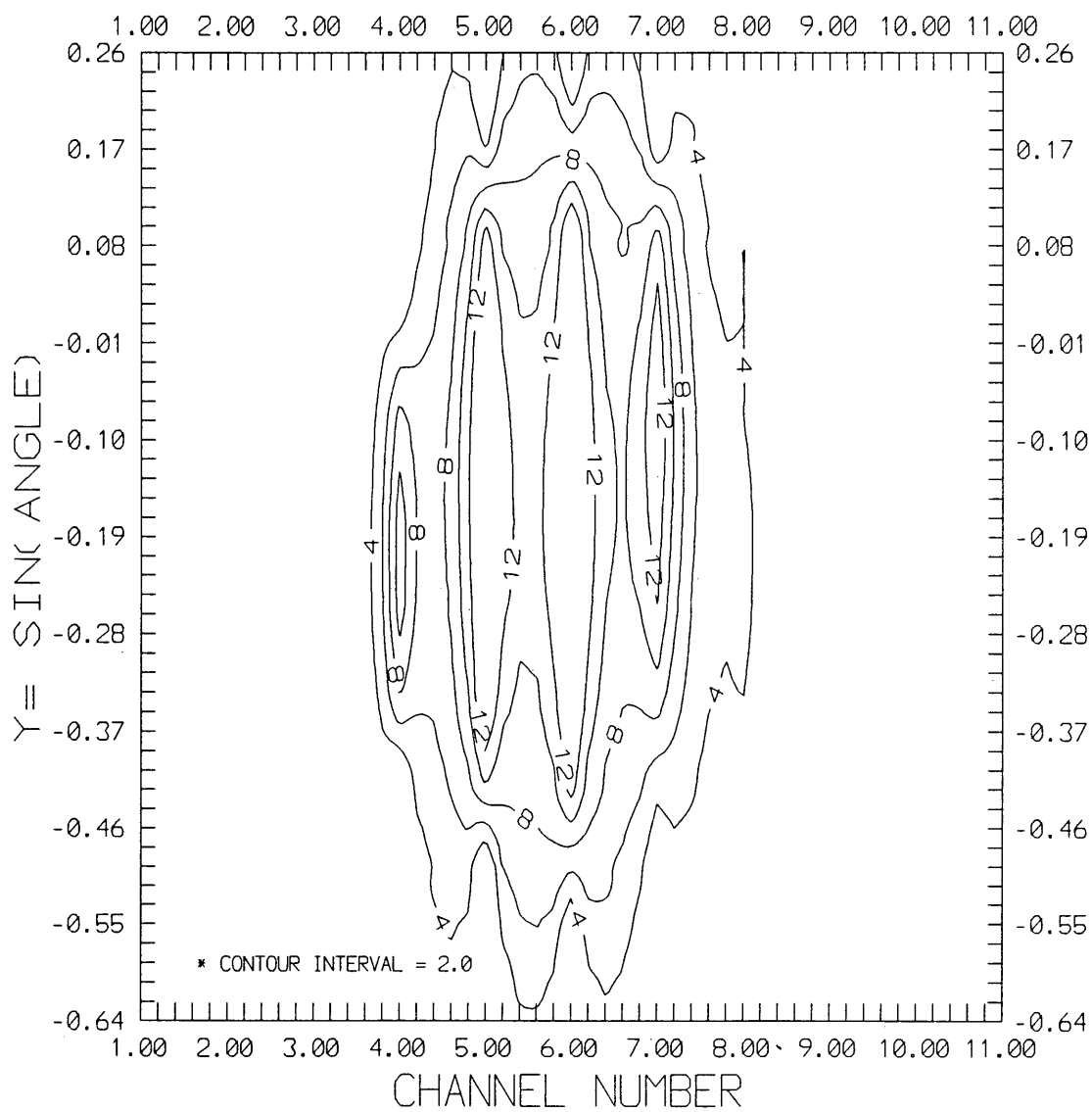


Figure 3-8. Beam Profile at 50 KV Accelerating Voltage
($V_g = 9.0$ KV)

Chapter IV

MODEL FITTING

4.1 Fitting Data to an Equation

From the study of previous chapter, we found that the relative intensity of the final beam profile is a multi-variable function which can be written as

$$D = D(E, V_a, V_g, x, y) \quad (4-1)$$

where E is the final energy of the particles, V_a is the accelerating voltage, V_g is the voltage of Grid Einzel lens, and, x and y are the coordinates at the target chamber.

Since the two lenses in the accelerator are Einzel lenses which increase and decrease the energy of particles in the same amount, we can write the final energy for a beam

$$E = Ze(V_{ex} + V_a)$$

where Ze is the total charge of the beam particle and V_{ex} is the voltage of Extraction Gap. In the case of our study, Z is one for photon beam and V_{ex} is 20 KV. Equation (4-1) now is simplified to

$$D = D(V_a, V_g, x, y) \quad (4-2)$$

Fitting the experimental data to Equation (4-2) is a complex problem. A correct working procedure should be made for solving the problem like this. The procedure that we will follow is listed below which indicates the work to be done and the decisions to be made at each stage.

The procedure of fitting:

Step 1. Objective

1. Estimate effects
2. Predict responses

Step 2. Construct Full Equation

1. Previous study results
2. Search for candidate equation

Step 3. Selection of Subsets of Variables

1. Sampling each individual variable in full equation
2. Study the variance of each variable
3. Combination of reasonable variables
4. Reduce of functional variables
5. Appropriate values of coefficients in linear or nonlinear functional form of each remaining variable
6. Finding useful estimate equation

Step 4. Final Predictor Equation

1. Adjusting all selected parameters
2. Minimizing the total square residual

Now, we follow the procedure to find our theoretical model of the final beam profile of the accelerator.

We have a total of 1408 sets of experimental data which we collected in the two experiments discussed in previous chapter. Each set of data contains five measurements which are V_a , V_g , x , y and D . In the general operation of the accelerator, for a certain accelerating voltage, we should have a certain V_g that gives the best beam profile regardless of adjusting V_g from down side or up side. The adjustable range of V_g should be symmetric around the its best position that leads a normal distribution of V_g at certain accelerating voltage V_a . Looking over the three dimensional plots in Chapter III, we also found that there is a more or less normal type distribution in the beam profile in both x and y directions. Since different V_g should also affect x and y parts, the Equation (4-2) becomes

$$D = D[V_g(V_a), x(V_a, V_g), y(V_a, V_g)] \quad (4-3)$$

If we assume variable $V_g = V_g(V_a)$ is independent of variable x and y , use the symbol N to represent the normal distribution, we have our full equation of the model

$$D = D_0 N(V_g) N(x, y) \quad (4-4)$$

where D_0 is the weighting constant which we called the scale

factor in the computer program (see Appendix B).

An n dimensional normal distribution can be determined completely by its weight point $(\mu_1, \mu_2, \dots, \mu_n)$ and λ matrix (see Appendix A). If we put the normal constants of $N(V_g)$ and $N(x, y)$ into a function $C(V_a, V_g)$, now the forms of $N(V_g)$ and $N(x, y)$ are

$$N(V_g) = C(V_a, V_g) \exp \left\{ -\frac{1}{2} \left[\frac{V_g - \mu(V_g)}{\sigma(V_g)} \right]^2 \right\} \quad (4-5)$$

$$N(x, y) = \exp \left\{ -\frac{1}{2(1-\rho_{xy}^2)} \left[\left(\frac{x - \mu(x)}{\sigma(x)} \right)^2 - 2\rho_{xy} \frac{x - \mu(x)}{\sigma(x)} \cdot \frac{y - \mu(y)}{\sigma(y)} + \left(\frac{y - \mu(y)}{\sigma(y)} \right)^2 \right] \right\} \quad (4-6)$$

where μ is the variable mean, σ^2 is the variable variance and ρ_{xy} ($|\rho_{xy}| \leq 1$) is the correlation coefficient between variable x and variable y . All μ s and σ s are functions of V_a and V_g .

Before studying $N(V_g)$ and $N(x, y)$, we set up convenient x-y coordinates. In the x-axis, the ceramic rod with eleven copper rings on, since each ring has the width of 1/8 inches separated from one another 1/32 inches, we let 5/32 inches be the unit of x . So x can be replaced by the channel number shown on the scope. If let the length of rotating arm on the

detector which is 3/4 inches be the unit of y , we can write y as $\sin\theta$ where θ is the angle from the center position of the detector. For all the calculations, we replace x and y by channel number n and $\sin\theta$.

Following the procedure Step 3, we studied the total 1408 set samples of $D(x)$, $D(y)$, and $D(V_g)$, in which other variables were kept as constants. We find our estimate model

$$N(V_g) = N_1(0) \exp\left\{-\frac{1}{2} \left[\frac{V_g - \mu_1(V_g)}{\sigma_1(V_g)}\right]^2\right\} \\ + N_2(0) \exp\left\{-\frac{1}{2} \left[\frac{V_g - \mu_2(V_g)}{\sigma_2(V_g)}\right]^2\right\} \quad (4-7)$$

$$N(n, \theta) = \exp\left\{-\frac{1}{2(1-\rho_{xy}^2)} \left[\left(\frac{n - \mu_x}{\sigma_x}\right)^2 - 2\rho_{xy} \frac{n - \mu_x}{\sigma_x} \cdot \frac{\sin\theta - \mu_y}{\sigma_y} + \left(\frac{\sin\theta - \mu_y}{\sigma_y}\right)^2\right]\right\} \quad (4-8)$$

where σ_x is given by

$$\sigma_x = \sigma_x(0) \exp\left\{-\frac{1}{2} \left[\frac{V_g - \mu(\sigma_x)}{\sigma(\sigma_x)}\right]^2\right\} \quad (4-9)$$

and

$$D_0 = 1.000$$

$$\rho_{xy} = 0.500$$

$$\mu_y = -0.2078$$

The remaining parameters in the model are regressed to the polynomials of V_a and V_g . The coefficients of these polynomials are listed in Table 4-1 and Table 4-2.

Based on the observation of Figure 3-5 and Figure 3-6, $N(V_g)$ contribution to the beam profile is not symmetric about its best setting which has a slow-rising front and fast-falling tail, we write $N(V_g)$ as combination of two normal distributions.

Table 4-1. Coefficients of Parameters in Estimate Model

| | CONSTANT | V_a ($\times 10^{-2}$) | V_a^2 ($\times 10^{-4}$) | V_a^3 ($\times 10^{-6}$) |
|--------------------|----------|----------------------------|------------------------------|------------------------------|
| $N_1(0)$ | 3.27800 | 19.1647 | -37.310 | 21.23 |
| $N_2(0)$ | 5.66341 | 40.7526 | -48.962 | 17.85 |
| $\mu_1(V_g)$ | 1.84860 | 11.1890 | -78.890 | 3.51 |
| $\mu_2(V_g)$ | 2.29971 | 12.4936 | 1.094 | - 0.66 |
| $\sigma_1(V_g)$ | 0.52050 | - 0.7460 | 10.417 | - 4.87 |
| $\sigma_2(V_g)$ | 0.18800 | 0.7380 | 3.160 | - 1.34 |
| $\sigma_x(0)$ | 2.29776 | - 1.5799 | 2.375 | - 0.91 |
| $\mu(\sigma_x)$ | 1.73580 | 10.7510 | - 3.813 | - 2.22 |
| $\sigma(\sigma_x)$ | 0.64759 | 1.2800 | 6.954 | - 0.23 |
| σ_y | 0.25551 | - 0.1972 | 0.502 | - 0.35 |

Table 4-2. Coefficients of μ_x in Estimate Model

| CONSTANT | $V_a(10^{-2})$ | $V_g(10^{-1})$ | $V_a^2(10^{-4})$ | $V_g^2(10^{-3})$ | $V_a V_g(10^{-3})$ |
|----------|----------------|----------------|------------------|------------------|--------------------|
| 6.51700 | 5.7621 | -4.8442 | -4.9774 | 12.476 | 1.9901 |

Adjusting all the parameters and minimizing the total square residual in the estimate model by the computer program, the final predictor model is achieved. The final predictor has the same form of the estimate model with different parameters where

$$D_0 = 1.585$$

$$\rho_{xy} = 0.062$$

$$\mu_y = -0.1989$$

and rest of them are listed in Table 4-3 and Table 4-4.

To test if our predictor model is reasonable approximation or good fit, we introduce a quantity, which represents the reliability of the model, R

$$R = 1 - \frac{\text{RTSR}}{\text{SF}} = 1 - \frac{\left\{ \sum_i [D_i(\text{FIT}) - D_i(\text{MEASURE})]^2 \right\}^{\frac{1}{2}}}{\sum_i D_i(\text{FIT})} \quad (4-10)$$

where RTSR is the square root of the total square residual and SF is the sum of function of the predictor model. Since RTSR reflects to the estimated standard deviation of the

Table 4-3. Coefficients of Parameters in Predictor Model

| | CONSTANT | $V_a (\times 10^{-2})$ | $V_a^2 (\times 10^{-4})$ | $V_a^3 (\times 10^{-6})$ |
|--------------------|----------|------------------------|--------------------------|--------------------------|
| $N_1(0)$ | 3.31266 | 18.8748 | -41.084 | 24.86 |
| $N_2(0)$ | 5.69437 | 40.3708 | -53.568 | 22.97 |
| $\mu_1(V_g)$ | 1.89867 | 11.0703 | -12.164 | 7.82 |
| $\mu_2(V_g)$ | 2.34978 | 12.9835 | - 0.565 | 0.04 |
| $\sigma_1(V_g)$ | 0.57057 | - 0.8734 | 5.921 | - 0.55 |
| $\sigma_2(V_g)$ | 0.23799 | 1.1534 | 4.090 | - 2.74 |
| $\sigma_x(0)$ | 2.34714 | - 1.9105 | 2.007 | 0.20 |
| $\mu(\sigma_x)$ | 1.78587 | 11.1331 | - 3.491 | -10.90 |
| $\sigma(\sigma_x)$ | 0.69766 | 1.7097 | 10.264 | 3.15 |
| σ_y | 0.28093 | - 0.3999 | 0.667 | - 0.35 |

Table 4-4. Coefficients of μ_x in Predictor Model

| CONSTANT | $V_a(10^{-2})$ | $V_g(10^{-1})$ | $V_a^2(10^{-4})$ | $V_g^2(10^{-3})$ | $V_a V_g(10^{-3})$ |
|----------|----------------|----------------|------------------|------------------|--------------------|
| 6.51838 | 6.0413 | -4.8170 | - 5.59 | 12.730 | 2.173 |

model, the bigger R is, the better fitting is achieved.

The computer program also can give several local models at certain operation conditions. The performances of the predictor models in different range of accelerating voltage

are listed in Table 4-5 where the data with * mark are produced by the local models.

Table 4-5. Performances of Predictor Models

| V_a (KV) | V_g (KV) | SF | RTSR | R(%) | SF* | RTSR* | R*(%) |
|------------|------------|--------|-------|------|--------|-------|-------|
| 0 | 2.5 | 303.55 | 23.03 | 92.4 | 374.56 | 17.52 | 95.3 |
| 25 | 6.0 | 335.21 | 23.10 | 93.1 | 395.77 | 17.36 | 95.6 |
| 50 | 9.0 | 487.69 | 24.81 | 94.9 | 395.34 | 17.54 | 95.6 |
| 75 | 13.5 | 341.83 | 21.47 | 93.7 | 398.36 | 18.49 | 95.4 |
| 100 | 17.0 | 396.01 | 17.49 | 95.6 | 375.31 | 17.01 | 95.5 |

4.2 Beam Profile Simulation

Using the predictor model, we can simulate the beam profile at any operation condition. Figure 4-1 to Figure 4-3 shows the relative intensity of the beam at 80 KV accelerating voltage.

From the model, we can predict the shape of beam spot and best voltage setting of the Grid Einzel Lens at required operation condition which is helpful information for designing the target and using the accelerator.

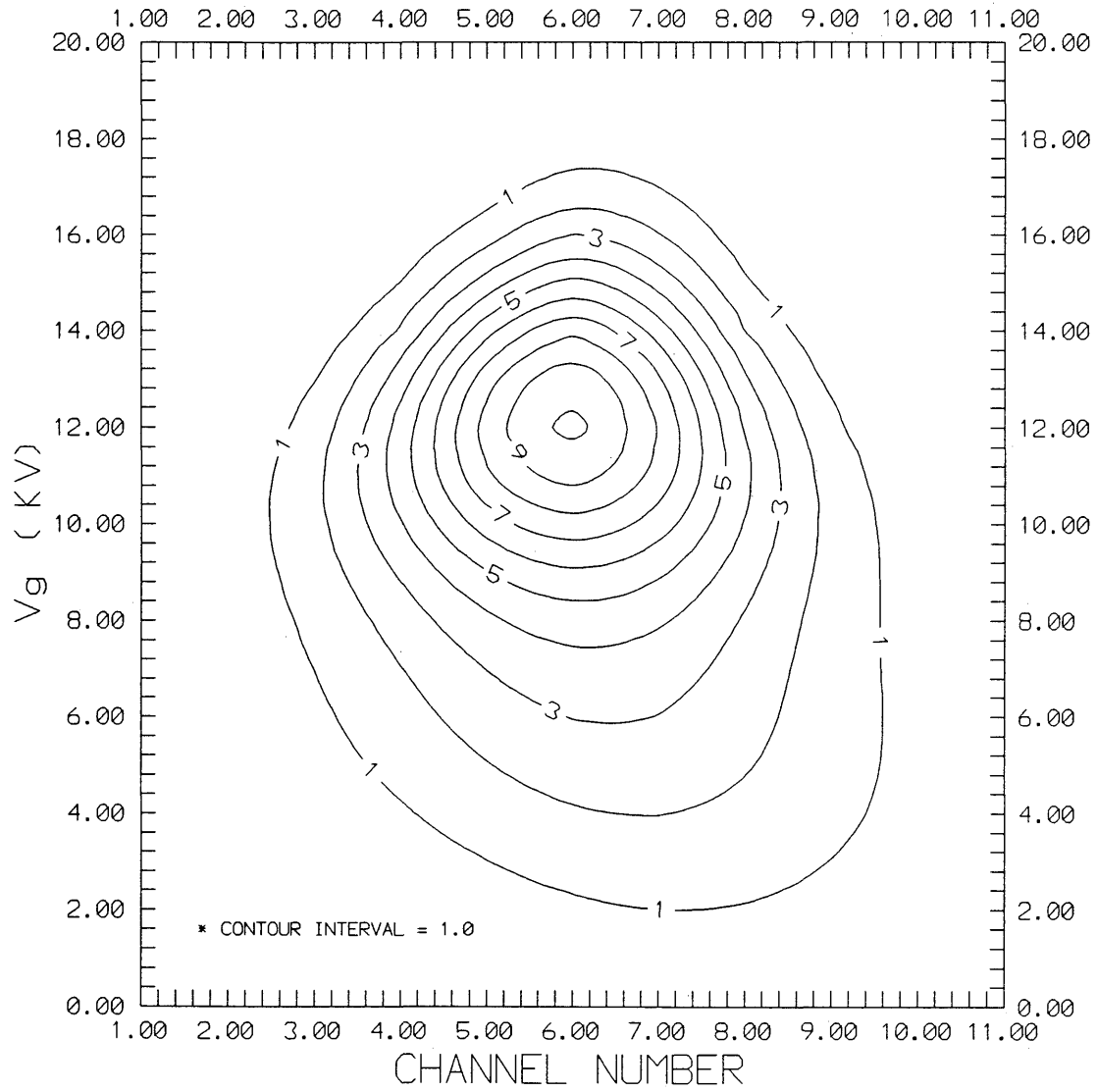


Figure 4-1. Relative Beam Intensity as Function of n and V_g at 80 KV Accelerating Voltage

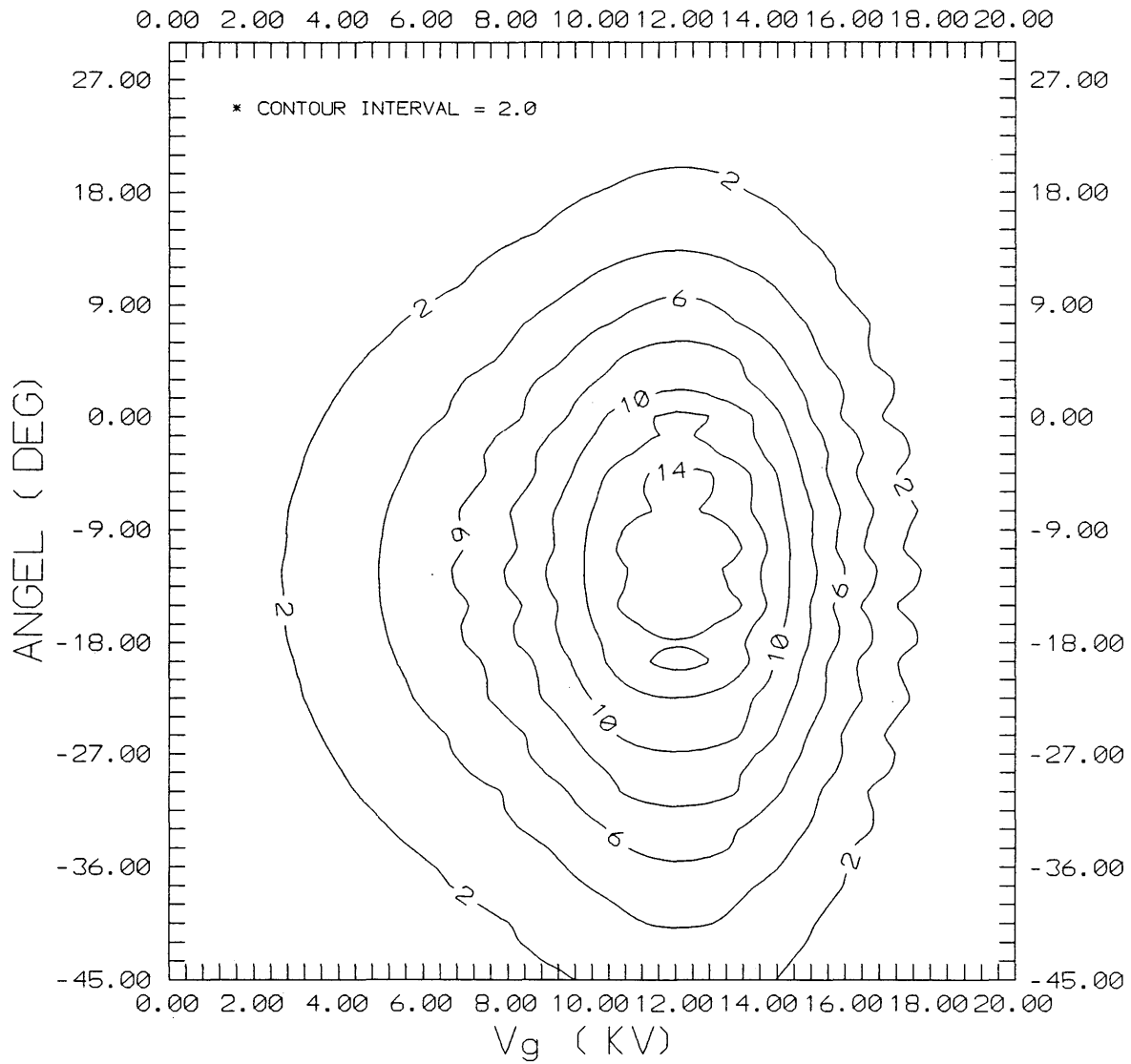


Figure 4-2. Relative Beam Intensity as Function of $\sin\theta$ and V_g at 80 KV Accelerating Voltage

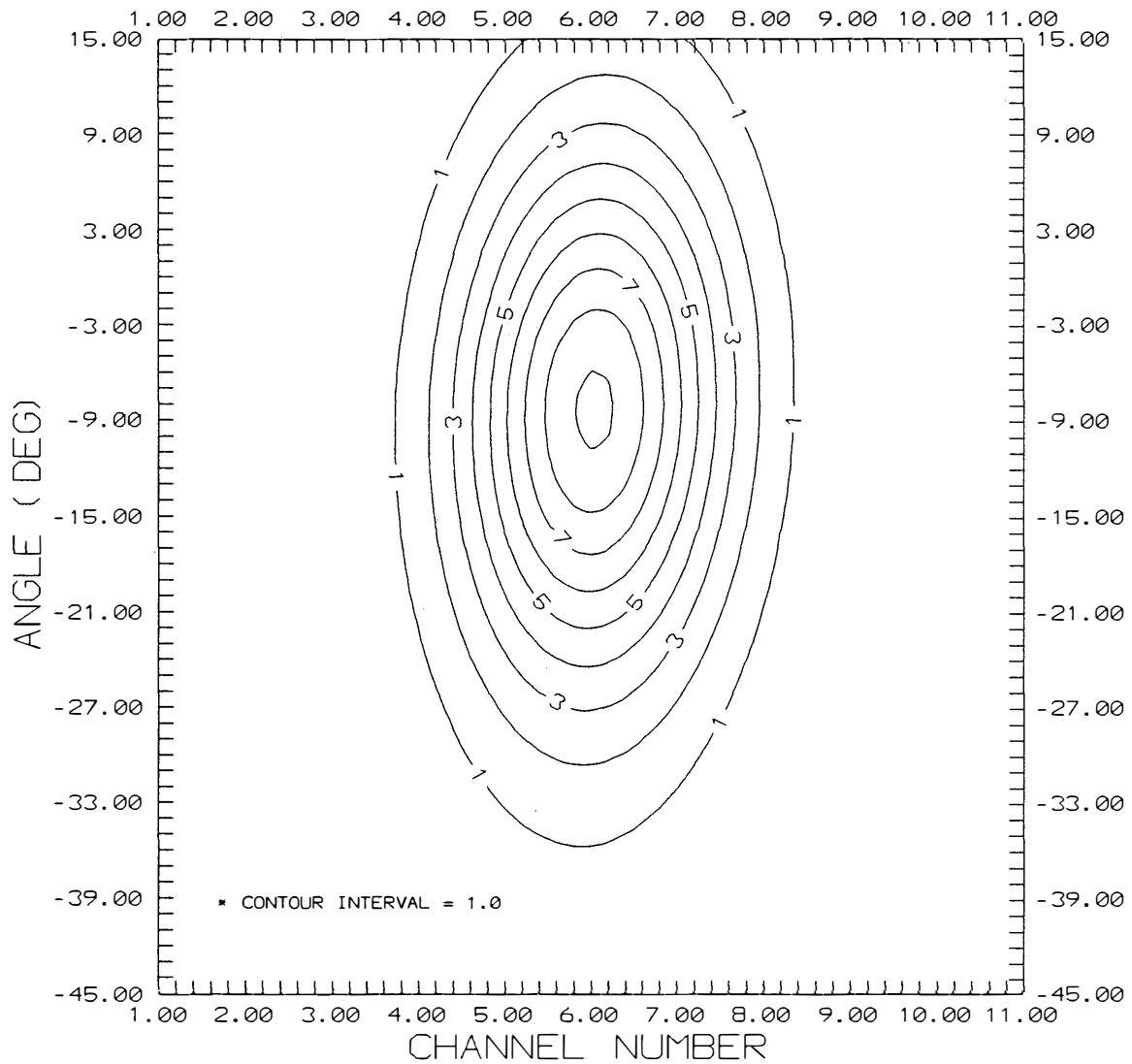


Figure 4-3. Beam Profile at 80 KV Accelerating Voltage
($V_g = 15$ KV)

Chapter V

COMPARISON

The predictor model developed in previous chapter is compared with a theoretical accelerator design program OPTICIAN [WH87], which is provided by the same accelerator manufacturer.

From OPTICIAN, we can get x and y coordinates after each element of the accelerator. An overall transfer matrix of the accelerator can be given by OPTICIAN at certain operating condition. Table 5-1 shows the output of OPTICIAN at 100 KV accelerating voltage and 17 KV voltage of GEL.

Assuming that the distribution of ions emitted from the ion source is a normal distribution of the emitting angle, fixing all other conditions at the same, a complete beam profile can be generated by using OPTICIAN. Figure 5-1 shows the beam profile pattern at 100 KV accelerating voltage and 17 KV voltage of GEL generated by using OPTICIAN.

The results from the predictor model agree well as the results given by OPTICIAN both in the shape and the size of beam patterns in the range of operation conditions.

The shapes of the beam patterns, having an elliptical shape in the contour plots, are found experimentally as shown in Figure 3-7 and theoretically as shown in Figure 4-3

Table 5-1. List Output of OPTICIAN at

$$V_a = 100 \text{ KV and } V_g = 17 \text{ KV}$$

File: COPARISON
 Title: COPARISON
 Created: Jun 5, 1990 3:33:15

```

Ion source 1 Momentum = 6.104 MeV/c Mass = 1.000 Charge = 1.
              Inj energy .020 MeV, Current = .300mA
Focal len. 2 X Focal L. 1.000m. Y Focal L. 1.000m.
              Energy = .020 MeV
Magnet       3 Radius = .229m. Bend angle 90.00 Fringe fld: .00900
              Beta1 = .000 Beta2 = .000
              Energy = .020MeV Field index .000 Field = .08891 T
Accel tube  4 Length = .600m. Ent dia = .070m. Voltage = .100MV
              Charge state 1. Inj energy .020MeV
              Ent lens 1 Exit lens 1
Focal len.  5 X Focal L. 1.200m. Y Focal L. 1.200m.
              Energy = .120 MeV
Drift        6 Length = 1.500 m.
              Energy = .120 MeV
    
```

COORDINATES AT END OF EACH ELEMENT:

| After element | | X mm., | X'mrad | Y mm. | Y'mrad | DeltaP/P % | DeltaL mm |
|---------------|--------|--------|--------|-------|--------|------------|-----------|
| Ion source | 1 Env. | 1.0 | 20.0 | 1.0 | 20.0 | .00 | .0 |
| Focal len. | 2 Env. | 1.0 | 20.0 | 1.0 | 20.0 | .00 | .0 |
| Magnet | 3 Env. | 4.6 | 4.3 | 7.3 | 22.6 | .00 | 4.7 |
| Accel tube | 4 Env. | 2.6 | 3.1 | 10.5 | 7.6 | .00 | 11.4 |
| Focal len. | 5 Env. | 2.6 | 3.8 | 10.5 | 1.4 | .00 | 11.4 |
| Drift | 6 Env. | 4.7 | 3.8 | 8.8 | 1.4 | .00 | 11.4 |

DISTANCE TO NEXT WAIST

TIME

| After element | | Xdist m | Ydist m | X mm., | Y mm. | microsec |
|---------------|---|---------|---------|--------|-------|----------|
| Ion source | 1 | .00 | .00 | 1.0 | 1.0 | .0000 |
| Focal len. | 2 | .00 | .00 | 1.0 | 1.0 | .0000 |
| Magnet | 3 | -.08 | -.32 | 4.6 | .9 | .1831 |
| Accel tube | 4 | -.02 | -1.37 | 2.6 | 1.1 | .3602 |
| Focal len. | 5 | .39 | 6.23 | 2.2 | 5.8 | .3602 |
| Drift | 6 | -1.10 | 4.74 | 2.2 | 5.9 | .6719 |

OVERALL TRANSFER MATRIX:

| | | | | | |
|---------|--------|---------|--------|--------|--------|
| -3.2594 | -.1692 | .0000 | .0000 | .6159 | .0000 |
| -1.0802 | -.1811 | .0000 | .0000 | .1059 | .0000 |
| .0000 | .0000 | -1.0188 | .4386 | .0000 | .0000 |
| .0000 | .0000 | -.7977 | -.0572 | .0000 | .0000 |
| .0000 | .0000 | .0000 | .0000 | .1667 | .0000 |
| 1.9222 | .5626 | .0000 | .0000 | 1.7198 | 2.4495 |

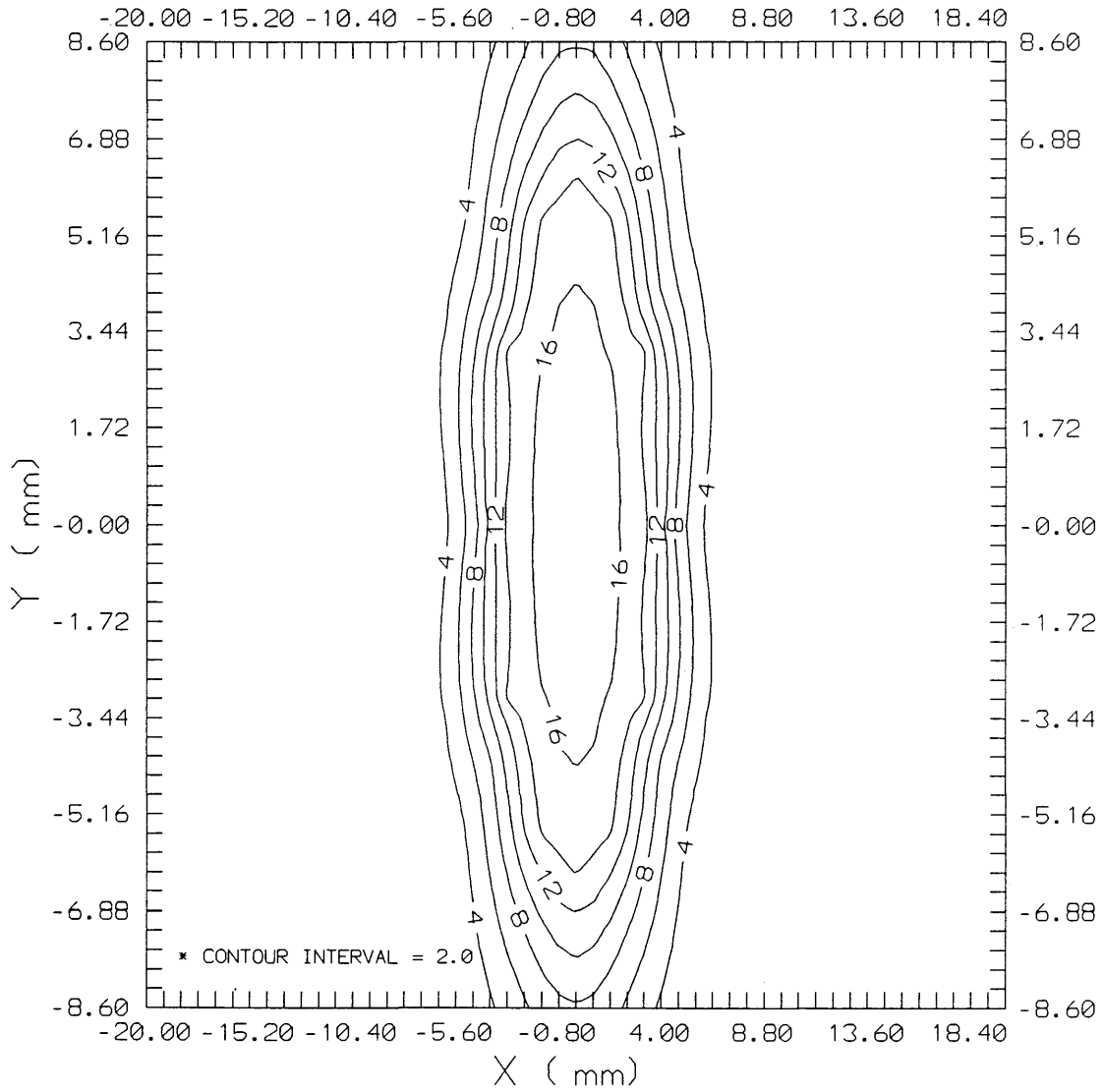


Figure 5-1. Beam Profile Generated by OPTICIAN at 100 KV Accelerating Voltage and 17 KV Voltage of GEL

and Figure 5-1. The y-semiaxis b is bigger than x-semiaxis a of the ellipse. We also found that b is more sensitive than a when the accelerating voltage and the voltage of GEL were changed.

The sizes of the beam patterns given by the predictor model and OPTICIAN are about the same. At 100 KV accelerating voltage, the beam spot, given by the predictor model, is about 0.96 cm x 1.41 cm and about 0.94 cm x 1.76 cm given by OPTICIAN.

From the above facts, we conclude that the predictor model is a useful tool to predict the shape and the size of beam patterns which is approximately as good and reliable as the beam optics result of the General Ionex Model 1545 Linear Particle Accelerator.

REFERENCE CITED

- [BA66] M. Bandford, "The Transport of Charged Particle Beam", Spon Books Ltd., London (1966).
- [CE89] F. E. Cecil, Private Communications.
- [GA89] A. Gaviria, "Beam Profile Monitor for a 150 KeV Linear Accelerator", Senior Thesis, Department of Physics, Colorado School of Mines, Golden, CO 80401 (1989).
- [GA84] J. E. Galvin and I. E. Brown, "Ion Beam Profile Monitor", Rev. Sci. Instr., 55(11), (1984) 1866 - 1867.
- [GE82] "Air Insulated Accelerator System Model 1545: Technical Specifications", General Ionex Corporation, 19 Graf Road, Newburyport, MA 01950 (1982).
- [LI69] J. J. Livingood, "The Optics of Dipole Magnets", Acad. Press, New York (1969).
- [WH87] N. R. White, "Computers and The Design of Ion Beam Optical System", Nucl. Instr. and Meth., B21 (1987) 339-349.

SELECTED BIBLIOGRAPHY

- [1] J. F. Ziegler and R. F. Level, eds., "Ion Implantation Equipment and Techniques:", North Holland (1985).
- [2] J. F. Ziegler, ed., "Ion Implantation: Science and Technology", 2ed., Acad. Press (1988).
- [3] J. Keller, "Beam Optics Design for Ion Implantation", Nucl. Instr. and Meth., 189 (1981) 7-14.
- [4] H. F. Glavish, "Magnet Optics for Beam Transport", Nucl. Instr. and Meth., 189 (1981) 43-53.
- [5] A. Septier, ed., "Focussing of Charged Particles Vol.1 and Vol.2", Acad. Press, New York (1967).
- [6] A. Septier, ed., "Applied Charged Particle Optics: Part C", Acad. Press, New York (1983).
- [7] H. Wollnik, "Optics of Charged Particles", Acad. Press, New York (1987).
- [8] A. J. Boerboom, " Ion Optics of Multipoles", Nucl. Instr. and Meth., A258 (1987) 426-430.
- [9] K. Oide, "A Final Focus System for Flat-Beam Linear Colliders", Nucl. Instr. and Meth., A276 (1989) 427-432.
- [10] M. Baril and M. Noel, "Modification of an Achromatic Mass Spectrometer to Include Transverse Focusing", Nucl. Instr. and Meth., A258 (1987) 318-322.

- [11] N. R. White and K. H. Purser, "The Design of Magnets with Nondipole Field Components", Nucl. Instr. and Meth., A258 (1987) 437-442.
- [12] H. Wollnik, J. Brezina and M. Berz, "Gios-Beam Trace: A Program Package to Determine Optics Properties of Intense Ion Beams", Nucl. Instr. and Meth., A258 (1987) 408-411.
- [13] G. W. Grime and J. Takacs, "An Ion Accelerator Facility for The Preparation of Nuclear Bombardment Targets", Nucl. Instr. and Meth., 189 (1981) 199-203.
- [14] T. Wada, N. Takahashi and I. Yamamoto, "Electron Beam Profile Measurement by Using TL Sheets", Nucl. Instr. and Meth., A261 (1987) 368-372.
- [15] R. R. Silbar, "Beam Ellipse Matching: Waist-to-Waist Transport", Nucl. Instr. and Meth., 87 (1970) 221-227.
- [16] K. S. Krane, "Introductory Nuclear Physics", Wiley, New York (1987).
- [17] J. D. Jackson, "Classical Electrodynamics", 2nd ed., Wiley, New York (1975).
- [18] R. Walpole and R. Myers, "Probability and Statistics for Engineers and Scientists", 4th ed., Macm. Pub. Co, New York (1989).

Appendix A
NORMAL DISTRIBUTION

The Normal Distribution is the most frequently used continuous probability distribution in the entire field of statistics. Its graph called the normal curve, is the bell shaped curve of Figure A-1.

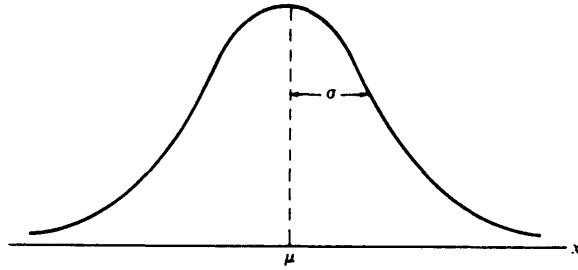


Figure A-1. Normal Curve

A continuous random variable X having the bell-shaped distribution of Figure A-1 is called a normal random variable. The mathematical equation for the probability distribution of the normal variable depends on the two parameters μ and σ , its mean and standard deviation

$$n(x; \mu, \sigma) = \frac{1}{(2\pi)^{\frac{1}{2}}\sigma} \exp \left\{ -\frac{1}{2} \left[\frac{x - \mu}{\sigma} \right]^2 \right\} \quad (\text{A-1})$$

Once μ and σ are specified, the normal curve is completely

determined.

The density function of n normal variable x_1, x_2, \dots, x_n can be written as

$$n(x_1, x_2, \dots, x_n) = \frac{1}{((2\pi)^n \det[\lambda_{ik}])^{\frac{1}{2}}} \exp \left\{ -\frac{1}{2} \sum_{i=1}^n \sum_{k=1}^n \lambda_{ik} (x_i - \mu_i)(x_k - \mu_k) \right\} \quad (\text{A-2})$$

where μ_i is the mean of x_i , λ_{ik} is the element of λ matrix (where $[\lambda] = [\Lambda]^{-1}$). The element of λ matrix is given

$$\lambda_{ik} = \begin{cases} E\{(x_i - \mu_i)^2\} = \text{Var}\{x_i\} = \sigma_i^2 & \text{if } i \neq k \\ E\{(x_i - \mu_i)(x_k - \mu_k)\} = \text{Cov}\{x_i, x_k\} & \text{if } i = k \end{cases}$$

When $n = 2$, Equation (A-2) becomes

$$n(x_1, x_2) = \frac{1}{2\pi\sigma_1\sigma_2(1-\rho_{12}^2)} \exp \left\{ -\frac{1}{2(1-\rho_{12}^2)} \left[\left(\frac{x_1 - \mu_1}{\sigma_1} \right)^2 - 2\rho_{12} \frac{x_1 - \mu_1}{\sigma_1} \cdot \frac{x_2 - \mu_2}{\sigma_2} + \left(\frac{x_2 - \mu_2}{\sigma_2} \right)^2 \right] \right\}$$

where ρ_{12} is called the correlation coefficient of x_1 and x_2 and given by

$$\rho_{12} = \rho_{21} = \frac{\lambda_{12}}{(\lambda_{11}\lambda_{22})^{\frac{1}{2}}} = \frac{\text{Cov}\{x_1, x_2\}}{(\text{Var}\{x_1\}\text{Var}\{x_2\})^{\frac{1}{2}}}$$

The normal distribution is often referred to as the Gaussian distribution, in honor of Karl Friedrich Gauss (1777-1855), who also derived its equation from a study of error in repeated measurements of the same quantity.

Generally, let x be a random variable with probability distribution $f(x)$. The mean or expected value and variance are

$$\mu = E\{x\} = \sum_i x_i f(x_i)$$

$$\sigma^2 = E\{(x-\mu)^2\} = \sum_i (x_i - \mu)^2 f(x_i)$$

if x is discrete, and

$$\mu = E\{x\} = \int_{-\infty}^{\infty} xf(x)dx$$

$$\sigma^2 = E\{(x-\mu)^2\} = \int_{-\infty}^{\infty} (x-\mu)^2 f(x)dx$$

if x is continuous.

The positive square root of variance, σ , is called the standard deviation of x .

Appendix B
FORTRAN PROGRAM

```

C ***** C
C Program of fitting four independent variables to a two C
C dimensional Normal distribution type equation with C
C multiple parameters. C
C ***** C
C Program written by: C
C Lian He C
C Department of Physics C
C Colorado School of Mines C
C ***** C
      INTEGER I, J, K, IMAX, JMAX, KMAX, JBEG, JEND
      PARAMETER (IMAX=5, JMAX=1408, KMAX=3)
      REAL DAT(IMAX,JMAX), CAL(KMAX,JMAX)
      REAL CNCOEF(4,6), SGCOEF(4,4), XMCOEF(6)
      REAL SSR, NSSR, RHO, SCALE, YMU
      COMMON JBEG, JEND, SFX, SCALFX, TRES, TSRES
      COMMON CNCOEF, SGCOEF, XMCOEF, RHO, SCALE, YMU
C Input the experimental data:
      CALL INPUT
C Select the fitting option:
      CALL OPTION

```

C Set the initial parameters of fitting model:

C Open CNCOEF.BAK, SGCOEF.BAK and XMCOEF.BAK for input:

```
      OPEN (UNIT=1, FILE='CNCOEF.BAK', FORM='FORMATTED',
*           STATUS='OLD')
      DO 10 J=1, 6
          READ (1,201) (CNCOEF(I,J), I=1, 4)
201     FORMAT (F8.5,1X,F9.6,1X,F10.7,1X,F11.8)
      10 CONTINUE
      CLOSE (1)
```

C

```
      OPEN (UNIT=1, FILE='SGCOEF.BAK', FORM='FORMATTED',
*           STATUS='OLD')
      DO 20 J=1, 4
          READ (1,202) (SGCOEF(I,J), I=1, 4)
202     FORMAT (F8.5,1X,F9.6,1X,F10.7,1X,F11.8)
      20 CONTINUE
      CLOSE (1)
```

C

```
      OPEN (UNIT=1, FILE='XMCOEF.BAK', FORM='FORMATTED',
*           STATUS='OLD')
      READ (1,203) (XMCOEF(I), I=1, 6)
203     FORMAT (6(F9.6,1X))
      CLOSE (1)
```

C

C Start adjusting parameters of fitting model:

RHO = 0.500

SCALE = 1.000

YMU = -0.2078

CALL CALCULATE (DAT,CAL)

SSR = TSRES

C

DO 140 K=1, 5000

IF (RHO .GT. 0.0 .AND. RHO .LT. 1.0) THEN

RHO = RHO + 0.001

CALL CALCULATE (DAT,CAL)

NSSR = TSRES

IF (NSSR .LT. SSR) THEN

SSR = NSSR

GOTO 30

ENDIF

RHO = RHO - 0.002

CALL CALCULATE (DAT,CAL)

NSSR = TSRES

IF (NSSR .LT. SSR) THEN

SSR = NSSR

GOTO 30

ENDIF

RHO = RHO + 0.001

```
        ENDIF
30 CONTINUE
C
    SCALE = SCALE + 0.001
    CALL CALCULATE (DAT,CAL)
    NSSR = TSRESD
    IF (NSSR .LT. SSR) THEN
        SSR = NSSR
        GOTO 40
    ENDIF
    SCALE = SCALE - 0.002
    CALL CALCULATE (DAT,CAL)
    NSSR = TSRESD
    IF (NSSR .LT. SSR) THEN
        SSR = NSSR
        GOTO 40
    ENDIF
    SCALE = SCALE + 0.001
40 CONTINUE
C
    YMU = YMU + 0.0001
    CALL CALCULATE (DAT,CAL)
    NSSR = TSRESD
    IF (NSSR .LT. SSR) THEN
```

```
        SSR = NSSR
        GOTO 50
ENDIF
YMU = YMU - 0.0002
CALL CALCULATE (DAT,CAL)
NSSR = TSRESO
IF (NSSR .LT. SSR) THEN
        SSR = NSSR
        GOTO 50
ENDIF
YMU = YMU + 0.0001
50 CONTINUE
```

C

```
DO 70 I=1, 6
XMCOEF(I) = XMCOEF(I) + 0.000001
CALL CALCULATE (DAT,CAL)
NSSR = TSRESO
IF (NSSR .LT. SSR) THEN
        SSR = NSSR
        GOTO 60
ENDIF
XMCOEF(I) = XMCOEF(I) - 0.000002
CALL CALCULATE (DAT,CAL)
NSSR = TSRESO
```

```
IF (NSSR .LT. SSR) THEN
    SSR = NSSR
    GOTO 60
ENDIF
XMCOEF(I) = XMCOEF(I) + 0.000001
60 CONTINUE
70 CONTINUE
```

C

```
DO 100 I=1, 4
DO 90 J=1, 4
SGCOEF(I,J) = SGCOEF(I,J) + 0.0001 * (0.1**I)
CALL CALCULATE (DAT,CAL)
NSSR = TSRES
IF (NSSR .LT. SSR) THEN
    SSR = NSSR
    GOTO 80
ENDIF
SGCOEF(I,J) = SGCOEF(I,J) - 0.0002 * (0.1**I)
CALL CALCULATE (DAT,CAL)
NSSR = TSRES
IF (NSSR .LT. SSR) THEN
    SSR = NSSR
    GOTO 80
ENDIF
```

```
      SGCOEF(I,J) = SGCOEF(I,J) + 0.0001 * (0.1**I)
80  CONTINUE
90  CONTINUE
100 CONTINUE
```

C

```
      DO 130 I=1, 4
      DO 120 J=1, 6
      CNCOEF(I,J) = CNCOEF(I,J) + 0.0001 * (0.1**I)
      CALL CALCULATE (DAT,CAL)
      NSSR = TSRESO
      IF (NSSR .LT. SSR) THEN
          SSR = NSSR
          GOTO 110
      ENDIF
      CNCOEF(I,J) = CNCOEF(I,J) - 0.0002 * (0.1**I)
      CALL CALCULATE (DAT,CAL)
      NSSR = TSRESO
      IF (NSSR .LT. SSR) THEN
          SSR = NSSR
          GOTO 110
      ENDIF
      CNCOEF(I,J) = CNCOEF(I,J) + 0.0001 * (0.1**I)
110 CONTINUE
120 CONTINUE
```

```
130 CONTINUE
C
    PRINT 204, K, RHO, SCALE, YMU, TRES D, SSR
204 FORMAT (2X,I5,2(4X,F5.3),4X,F7.4,2(4X,F12.5))
140 CONTINUE
C Print out the result:
    CALL OUTPUT (DAT,CAL)
C
    STOP
    END
C
C
    SUBROUTINE OPTION (JBEG,JEND)
C Select the experimental data to be used in fitting model:
    INTEGER OPNUM
    PRINT *, 'All experimental data were collected at:'
    PRINT *, 'Voltage (Extraction Gap) = 20 KV'
    PRINT *, 'Voltage (1st Einzel Lens) = 15 KV'
    PRINT *, 'There are 13 options listed below:'
    PRINT *, ' Option 1: V(Acc) = 0 KV, Angle = 0 DEG'
    PRINT *, ' Option 2: V(Acc) = 25 KV, Angle = 0 DEG'
    PRINT *, ' Option 3: V(Acc) = 50 KV, Angle = 0 DEG'
    PRINT *, ' Option 4: V(Acc) = 75 KV, Angle = 0 DEG'
    PRINT *, ' Option 5: V(Acc) = 100 KV, Angle = 0 DEG'
```

```
PRINT *, ' Option 6: V(Acc) = 0 KV, VGEL = 2.5 KV'  
PRINT *, ' Option 7: V(Acc) = 25 KV, VGEL = 6.0 KV'  
PRINT *, ' Option 8: V(Acc) = 50 KV, VGEL = 9.0 KV'  
PRINT *, ' Option 9: V(Acc) = 75 KV, VGEL = 13.5 KV'  
PRINT *, ' Option 10: V(Acc) = 100 KV, VGEL = 17.0 KV'  
PRINT *, ' Option 11: All data of option 1 to 5 '  
PRINT *, ' Option 12: All data of option 6 to 10 '  
PRINT *, ' Option 13: All experimental data'
```

C Enter the option number:

```
PRINT '(/'  
PRINT *, 'Enter the option number (1 to 13):'  
PRINT *, 'OPTION NUMBER = ? '  
READ *, OPNUM
```

C

```
IF (OPNUM .EQ. 1) THEN  
    PRINT *, 'OPTION 1: VGEL = 1.0 - 3.0 KV'  
    JBEG = 0  
    JEND = 55  
ELSE IF (OPNUM .EQ. 2) THEN  
    PRINT *, 'OPTION 2: VGIL = 2.0 - 6.5 KV'  
    JBEG = 55  
    JEND = 110  
ELSE IF (OPNUM .EQ. 3) THEN  
    PRINT *, 'OPTION 3: VGIL = 1.0 - 11.0 KV'
```

```
JBEG = 165
JEND = 121
ELSE IF (OPNUM .EQ. 4) THEN
  PRINT *, 'OPTION 4: VGIL = 0.0 - 15.0 KV'
  JBEG = 286
  JEND = 176
ELSE IF (OPNUM .EQ. 5) THEN
  PRINT *, 'OPTION 5: VGIL = 0.0 - 20.0 KV'
  JBEG = 462
  JEND = 231
ELSE IF (OPNUM .EQ. 6) THEN
  PRINT *, 'OPTION 6: ANGLE = -55 - 20 DEG'
  JBEG = 693
  JEND = 176
ELSE IF (OPNUM .EQ. 7) THEN
  PRINT *, 'OPTION 7: ANGLE = -45 - 15 DEG'
  JBEG = 869
  JEND = 143
ELSE IF (OPNUM .EQ. 8) THEN
  PRINT *, 'OPTION 8: ANGLE = -40 - 15 DEG'
  JBEG = 1012
  JEND = 132
ELSE IF (OPNUM .EQ. 9) THEN
  PRINT *, 'OPTION 9: ANGLE = -40 - 15 DEG'
```

```
JBEG = 1144
JEND = 132
ELSE IF (OPNUM .EQ. 10) THEN
  PRINT *, 'OPTION 10: ANGLE = -40 - 15 DEG'
  JBEG = 1276
  JEND = 132
ELSE IF (OPNUM .EQ. 11) THEN
  PRINT *, 'OPTION 11: V(Acc) = 0 - 100 KV,
*           VGIL = 0.0 - 20.0 KV'
  JBEG = 0
  JEND = 693
ELSE IF (OPNUM .EQ. 12) THEN
  PRINT *, 'OPTION 12: V(Acc) = 0 - 100 KV,
*           ANGLE = -55 - 20 DEG'
  JBEG = 693
  JEND = 715
ELSE
  PRINT *, 'OPTION 13 is selected'
  PRINT *, 'V(Acc) = 0 - 100 KV, VGIL = 0.0 - 20.0 KV
*           ANGLE = -55 - 20 DEG'
  JBEG = 0
  JEND = 1408
ENDIF
```

```
        RETURN
      END

C
C
      SUBROUTINE INPUT (DAT)
C Input the experimental data
C Input Arguments:
C DAT(I,J) - The array of experimental data
C DAT(1,J) - The channel number of the detector
C DAT(2,J) - The accelerating voltage
C DAT(3,J) - The voltage of Grid Einzel Lens (VGEL)
C DAT(4,J) - The angle from X - direction
C DAT(5,J) - The output voltage from the detector
      PARAMETER (IMAX=5, JMAX=1408)
      REAL DAT (IMAX,JMAX)
C Open file EXPT.DAT for input:
      OPEN (UNIT=1, FILE='EXPT.DAT', FORM='FORMATTED',
*          STATUS='OLD')
C Read each record:
      DO 10 J= 1, JMAX
      READ (1,101) (DAT(I,J), I=1, IMAX)
101  FORMAT (5(F5.1,1X))
      10 CONTINUE
C End-of-file reached
```

```

        CLOSE (1)

C
      RETURN

      END

C
C
      SUBROUTINE CALCULATE (DAT,CAL)
C Calculate the fitting model:
      PARAMETER (IMAX=5, JMAX=1408, KMAX=3)
      REAL DAT(IMAX,JMAX), CAL(KMAX,JMAX)
      REAL SFX, SCALFX, TRES D, TSRES D
      COMMON JBEG, JEND, SFX, SCALFX, TRES D, TSRES D
      COMMON CNCOEF, SGCOEF, XMCOEF, RHO, SCALE, YMU
      DATA PI/3.1415926/
C Set initial parameters:
      CO = 1/SQRT(1 - RHO**2)
      TRES D = 0.0
      TSRES D = 0.0
      SFX = 0.0
      SCALFX = 0.0
C Calculate the N(ACCV):
      DO 10 J=1, JEND
      CC1 = CNCOEF(1,1) + CNCOEF(2,1) * DAT(2,J+JBEG)
*           + CNCOEF(3,1) * (DAT(2,J+JBEG)**2)

```

```

*           + CNCOEF(4,1) * (DAT(2,J+JBEG)**3)
CC2 = CNCOEF(1,2) + CNCOEF(2,2) * DAT(2,J+JBEG)
*           + CNCOEF(3,2) * (DAT(2,J+JBEG)**2)
*           + CNCOEF(4,2) * (DAT(2,J+JBEG)**3)
CMU1 = CNCOEF(1,3) + CNCOEF(2,3) * DAT(2,J+JBEG)
*           + CNCOEF(3,3) * (DAT(2,J+JBEG)**2)
*           + CNCOEF(4,3) * (DAT(2,J+JBEG)**3)
CMU2 = CNCOEF(1,4) + CNCOEF(2,4) * DAT(2,J+JBEG)
*           + CNCOEF(3,4) * (DAT(2,J+JBEG)**2)
*           + CNCOEF(4,4) * (DAT(2,J+JBEG)**3)
CSGM1 = CNCOEF(1,5) + CNCOEF(2,5) * DAT(2,J+JBEG)
*           + CNCOEF(3,5) * (DAT(2,J+JBEG)**2)
*           + CNCOEF(4,5) * (DAT(2,J+JBEG)**3)
CSGM2 = CNCOEF(1,6) + CNCOEF(2,6) * DAT(2,J+JBEG)
*           + CNCOEF(3,6) * (DAT(2,J+JBEG)**2)
*           + CNCOEF(4,6) * (DAT(2,J+JBEG)**3)

```

C

```

N = CC1 * EXP(-0.5*((DAT(3,J+JBEG)-CMU1)/CSGM1)**2))
*       + CC2 * EXP(-0.5*((DAT(3,J+JBEG)-CMU2)/CSGM2)**2))

```

C Calculate MU(x):

```

XMU = XMCOEF(1) + XMCOEF(2) * DAT(2,J+JBEG)
*     + XMCOEF(3) * DAT(3,J+JBEG) + XMCOEF(4)
*     (DAT(2,J+JBEG)**2) + XMCOEF(5) * (DAT(3,J+JBEG)**2)
*     + XMCOEF(6) * DAT(2,J+JBEG) * DAT(3,J+JBEG)

```

C Calculate SIGMA(x):

```

XSGMC = SGCOEF(1,1) + SGCOEF(2,1) * DAT(2,J+JBEG)
*
*           + SGCOEF(3,1) * (DAT(2,J+JBEG)**2)
*
*           + SGCOEF(4,1) * (DAT(2,J+JBEG)**3)
XSGMMU = SGCOEF(1,2) + SGCOEF(2,2) * DAT(2,J+JBEG)
*
*           + SGCOEF(3,2) * (DAT(2,J+JBEG)**2)
*
*           + SGCOEF(4,2) * (DAT(2,J+JBEG)**3)
XSGMSGM = SGCOEF(1,3) + SGCOEF(2,3) * DAT(2,J+JBEG)
*
*           + SGCOEF(3,3) * (DAT(2,J+JBEG)**2)
*
*           + SGCOEF(4,3) * (DAT(2,J+JBEG)**3)

```

C

```

XSIGMA = XSGMC * EXP(-0.5*((DAT(3,J+JBEG)-XSGMMU)/
*
*           XSGMSGM)**2))

```

C Calculate SIGMA(y):

```

YSIGMA = SGCOEF(1,4) + SGCOEF(2,4) * DAT(2,J+JBEG)
*
*           + SGCOEF(3,4) * (DAT(2,J+JBEG)**2)
*
*           + SGCOEF(4,4) * (DAT(2,J+JBEG)**3)

```

C Calculate the fitting model:

```

PIJX = (DAT(1,J+JBEG) - XMU) / XSIGMA
PIJY = (SIN(PI*DAT(4,J+JBEG)/180) - YMU) / YSIGMA
PIJ = -0.5 * (C0**2) * (PIJX**2 - 2*RHO*PIJX*PIJY
*
*           + PIJY**2)
CALIJ = SCALE * N * EXP(PIJ)

```

C Set up CAL(I,J) array and calculate the sums:

```
      CAL(1,J+JBEG) = CALIJ
      CAL(2,J+JBEG) = CAL(1,J+JBEG) - DAT(5,J+JBEG)
      CAL(3,J+JBEG) = CAL(2,J+JBEG)**2
      TRES D = TRES D + ABS(CAL(2,J+JBEG))
      TSRES D = TSRES D + CAL(3,J+JBEG)
      SFX = SFX + DAT(5,J+JBEG)
      SCALFX = SCALFX + CAL(3,J+JBEG)
      IF (CAL(1,J+JBEG) .GT. 15.0) THEN
          CAL(1,J+JBEG) = 15.0
      ENDIF
10 CONTINUE

C
      RETURN
      END

C
C
      SUBROUTINE OUTPUT (DAT,CAL)
C Output the calculated data:
C Output argument:
C DAT(I,J) - The array of experimental data
C DAT(1,J) - The channel number of the detector
C DAT(2,J) - The accelerating voltage
C DAT(3,J) - The voltage of Grid Einzel Lens (VGEL)
C DAT(4,J) - The angle from X - direction
```

```
C DAT(5,J) - The output voltage from the detector
C CAL(I,J) - The array of calculated data
C CAL(1,J) - The fitted data of DAT(5,J)
C CAL(2,J) - Residual of fitted data
C CAL(3,J) - Square residual of fitted data
      PARAMETER (IMAX=5, JMAX=1408, KMAX=3)
      REAL DAT(IMAX,JMAX), CAL(KMAX,JMAX)
      COMMON JBEG, JEND, SFX, SCALFX, TRES, TSRES
      COMMON CNCOEF, SGCOEF, XMCOEF, RHO, SCALE, YMU
C Open file FIT.DAT for output:
      OPEN (UNIT=4, FILE='FIT.DAT', FORM='FORMATTED',
*           -STATUS='NEW')
C Store and print each record:
      WRITE (4,101) 'LIST OF OUTPUT'
      PRINT 101, 'LIST OF OUTPUT'
101 FORMAT (//,30X,A16,/)
      WRITE (4,102) 'CHNUM', 'ACCVOLT', 'VGEL', 'ANGLE',
*           'OUTVOLT', 'CALOUTV', 'RESID', 'SRESID'
      PRINT 102, 'CHNUM', 'ACCVOLT', 'VGEL', 'ANGLE',
*           'OUTVOLT', 'CALOUTV', 'RESID', 'SRESID'
102 FORMAT (/,2X,8(A8,2X),/)
C
      DO 10 J=1, JEND
          WRITE (4,103) (DAT(I,J), I=1, IMAX),
```

```

*           (CAL(K,J), K=1, KMAX)
      PRINT 103, (DAT(I,J), I=1, IMAX),
*           (CAL(K,J), K=1, KMAX)
103  FORMAT (2X,8(F8.2,2X))
10  CONTINUE
      WRITE (4,104) 'TOTALRES D = ', TRES D, 'TOTALSRES D = ',
*           TSRES D, 'CORR. COEF. = ', RHO
      PRINT 104, 'TOTALRES D = ', TRES D, 'TOTALSRES D = ',
*           TSRES D, 'CORR. COEF. = ', RHO
104  FORMAT (/ ,4X,A12,F10.5,4X,A13,F11.5,4X,A14,F5.3)
      WRITE (4,105) 'SUM[F(X)] = ', SFX, 'SUM[CAL(X)] = ',
*           SCALFX
      PRINT 105, 'SUM[F(X)] = ', 'SFX, 'SUM[CAL(X)] = ',
*           SCALFX
105  FORMAT (/ ,4X,A12,F8.2,4X,A15,F8.2)
      WRITE (4,106) 'SCALE = ', SCALE, 'YMU = ', YMU
      PRINT 106, 'SCALE = ', SCALE, 'YMU = ', YMU
106  FORMAT (/ ,4X,A8,F5.3,4X,A6,F7.4)
C Close file FIT.DAT:
      ENDFILE (4)
      CLOSE (4)
C Open file COEF.DAT for output:
      OPEN (UNIT=5, FILE='COEF.DAT', FORM='FORMATTED',
*           STATUS='NEW')

```

C Write N(ACCV), MU(X), SIGMA(X) and SIGMA(Y) coefficients:

```
      WRITE (5,107) 'COEFFICIENTS OF N(ACCV) '  
107  FORMAT (/,10X,A24,/  
      DO 20 J=1, 6  
          WRITE (5,108) (CNCOEF(I,J), I=1, 4)  
108  FORMAT (4X,F8.5,2X,F9.6,2X,F10.7,2X,F11.8)  
      20 CONTINUE  
      WRITE (5,107) 'COEFFICIENTS OF MU(X) '  
          WRITE (5, 109) (XMCOEF(I), I=1, 6)  
109  FORMAT (4X,6(F9.6,2X))  
      WRITE (5,107) 'COEFFICIENTS OF SIGMA(X) '  
      DO 30 J=1, 3  
          WRITE (5,110) (SGCOEF(I,J), I=1, 4)  
110  FORMAT (4X,F8.5,2X,F9.6,2X,F10.7,2X,F11.8)  
      30 CONTINUE  
      WRITE (5,107) 'COEFFICIENTS OF SIGMA(Y) '  
          WRITE (5,111) (SGCOEF((I,4), I=1, 4)  
111  FORMAT (4X,F8.5,2X,F9.6,2X,F10.7,2X,F11.8)
```

C Close file COEF.DAT:

```
      ENDFILE(5)
```

```
      CLOSE (5)
```

C

```
      RETURN
```

```
      END
```